CHAPTER 4

Antiplasmodial Activity of *Oncosiphon piluliferum*

4.1 *Oncosiphon piluliferum*

The historical name of this plant is *Pentzia globifera* and it belongs to the botanical family *Asteraceae*. The Europeans administered an infusion of the plant for convulsions and the Hottentots used an infusion of the flower and leaf for typhoid and other fevers. A decoction of the plant is an old fashioned "Dutch" remedy to bring out the rash in measles and both the Xhosa and Mfengu use it as an antifebrile. Extracts of the plant are reported to have given "negative results in experimental malaria".[1]

The plant is very bitter and has a "heavy smell" from the volatile oil which it contains; hence its common name stinkkruid. It is a bushy annual herb with stalkless leaves deeply dissected with two stipule-like lobes at the base and the flower heads sit on solitary long erect leaveless stalks. It grows mainly in the Witwatersrand region but also occurs in the Eastern Cape.

Figure 4.1 *Oncosiphon piluliferum* growing in Graaff-Reinet. Photo by Jean Meyer (SANBI)

[1] J.M. Watt and M.G. Breyer-Brandwyk, 'The Medicinal and Poisonous Plants of Southern and Eastern Africa', 2nd edition, Livingston, London, 1962, 254.

There are no reports on the chemical components of this plant to date. Chemical investigation of other *Pentzia* species has identified acetylenes, glaucolides, fulvenoguaianolides and other sesquiterpene lactones as constituents.[2]

4.2 *In vitro* Antiplasmodial Activity of *O. piluliferum* Extracts

A dichloromethane and a 1:1 dichloromethane/methanol extract were prepared from the aerial parts of the *O. piluliferum* plant (Table 4.1).

Table 4.1 Yield of extracts obtained from *O. piluliferum*

Extract Code	Extract description	% Yield
P01609A	Dichloromethane	2.2
P01609B	Dichloromethane/methanol (1:1)	3.3

The concentrated *O. piluliferum* extracts were tested *in vitro* in duplicate against a chloroquine-sensitive strain (D10) and the active dichloromethane extract was tested against the chloroquine-resistant (K1) strain of *P. falciparum*. (Table 4.2)

Table 4.2 *In vitro* antiplasmodial activity of *O. piluliferum* extracts

Extract	D10 (Experiment 1) IC_{50} (μg/ml)	D10 (Experiment 2) IC_{50} (μg/ml)	K1 IC_{50} (μg/ml)
P01609A	2.0	1.0	2.0
P01609B	>10	10.0	

The dichloromethane extract, P01609A, was found to be significantly active against both strains of the parasite having a 50% inhibitory concentration (IC_{50}) value of 2 μg/ml against the chloroquine-resistant (K1) strain. The 1:1 dichloromethane/methanol extract was found to be relatively inactive.

A bulk collection of plant material was undertaken to produce sufficient dichloromethane extract for bioassay-guided fractionation. This extract was bioassayed against the D10 strain and its activity (Table 4.3) compared favourably with that observed for the original extract.

[2] C. Zdero and F. Bohlmann, *Phytochemistry*, 1990, **29**, 189.

Table 4.3 *In vitro* antiplasmodial activity of extract of bulk plant material

Extract	D10 (Experiment 1) IC_{50} (μg/ml)	D10 (Experiment 2) IC_{50} (μg/ml)
P01609A (bulk)	2.6	3.1

4.3 Bioassay-guided Fractionation of the *O. piluliferum* Dichloromethane Extract

Bioassay-guided fractionation techniques based on antiplasmodial activity were used to identify and isolate the active compounds from the dichloromethane extract of *O. piluliferum*. Details of the purification techniques are given in Chapter 5 (Experimental).

4.3.1 Primary Fractionation of P01609A

Primary fractionation of the crude dichloromethane extract (P01609A) of O. *piluliferum* yielded a total of 32 pooled fractions. These fractions were bioassayed against *P. falciparum* D10. Due to difficulties experienced with the solubility of and the poor activity observed for the first 12 fractions these results were disregarded. The IC_{50} values for the remaining 20 fractions (7A - 7T) are summarised in Figure 4.2. Enhanced antiplasmodial activity was observed primarily in the region of fractions 7H - 7P. The identification of the compounds responsible for the observed activity is best illustrated by the further purification of fractions 7I, 7M and 7O. Further purification of the other active fractions resulted in the loss of observed antiplasmodial activity or pointed to the same active compounds.

4.3.2 Further Purification of Fraction 7I

Figure 4.3 summarizes the steps employed to further purify fraction 7I, guided by observed antiplasmodial activity against the D10 *P. falciparum* strain. Only fraction 8D was found to retain the activity of the parent fraction, 6I. Further fractionation of 8D led to the identification of a semi-pure compound, 9B, with enriched antiplasmodial activity. The compound was easily discernible on TLC by its characteristic dark pink colour when sprayed with vanillin spray reagent. Further purification of 9B yielded compound **(59).**

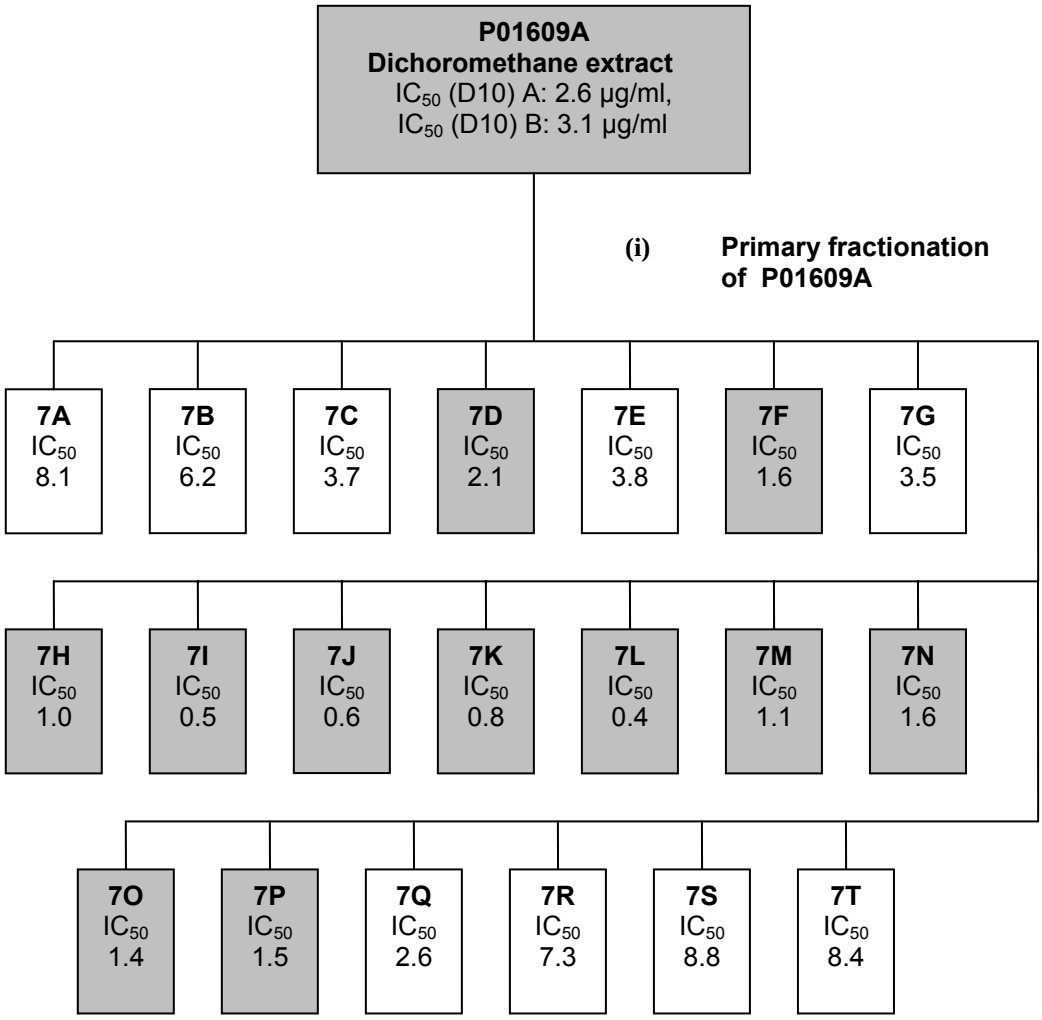

Figure 4.2 Summary of IC_{50} values of the primary fractions generated from silica gel column chromatography of P01609A. IC_{50} values are in µg/ml.

This compound, however, proved to be unstable and decomposed during NMR analysis, providing insufficient data for complete structural elucidation. Due to the observed instability of **(59)** and its low yield it was decided that a targeted purification of this compound from an adequate quantity of crude extract would be more practical than trying to re-isolate it from existing fractions containing minimal traces of it.

4.3.3 Further Purification of Fraction 7M

Figure 4.4 summarizes the steps employed to further purify fraction 7M. The crystalline fraction 11A was identified as the major constituent of 7M and was submitted for bioassaying. NMR Analysis of 11A, however, revealed that it was a

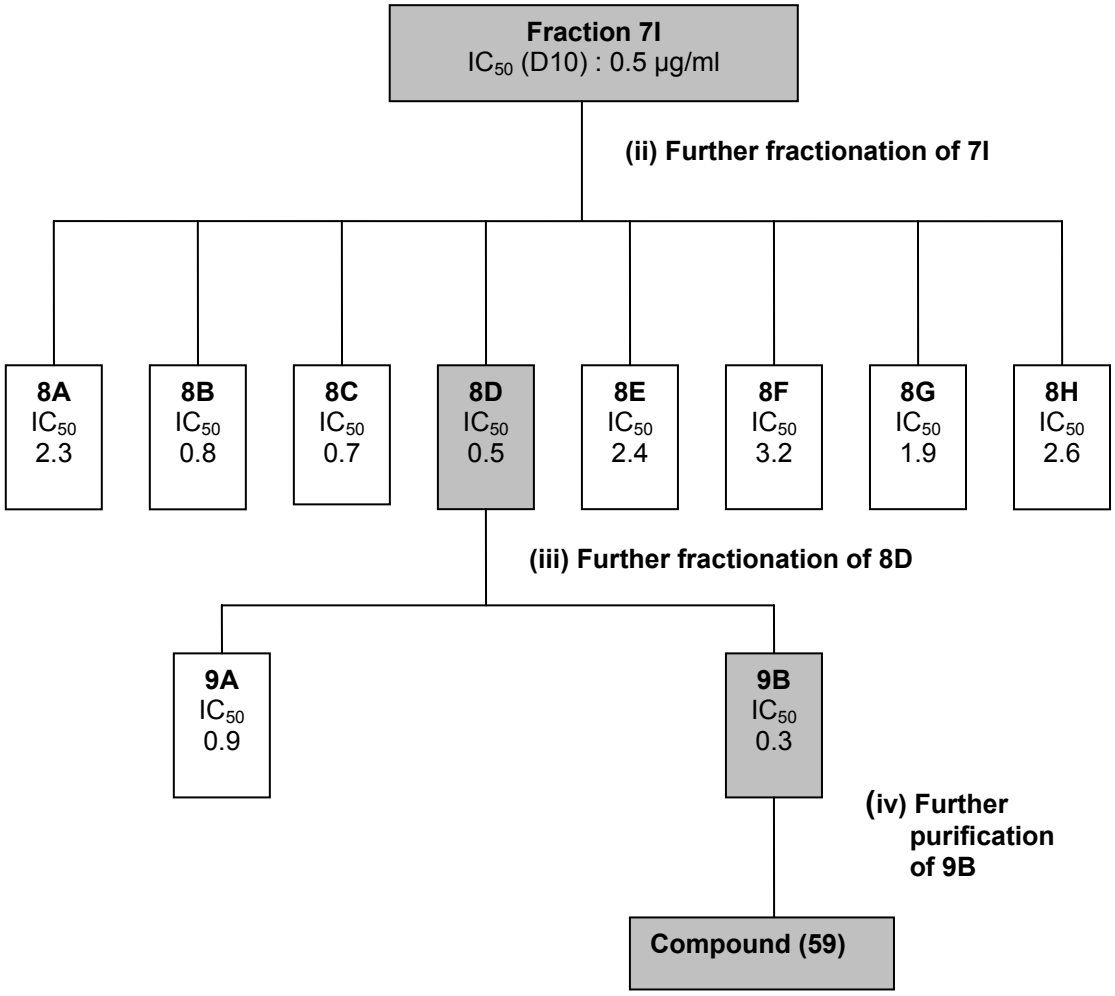

Figure 4.3 Further purification of fraction 7I. IC_{50} values are in µg/ml.

mixture of at least two closely related compounds. Further purification of 11A led to the isolation of the crystalline compound **(60)**, which had a characteristic blue-grey colour on TLC with vanillin spray reagent. The crystalline fraction 12A was found to contain a trace quantity of a closely related compound **(61)** and a major compound **(62)**. Despite their very close R_f values on TLC, compound **(61)** and **(62)** could be distinguished by their respective brown and pink colours when sprayed with vanillin reagent. The yield of 12A was too low to attempt the difficult purification required to separate compounds **(61)** and **(62)** with the aim of isolating sufficient quantities of each for structural elucidation and bioassaying. Thus, a targeted purification of these compounds from a larger quantity of crude extract was opted for.

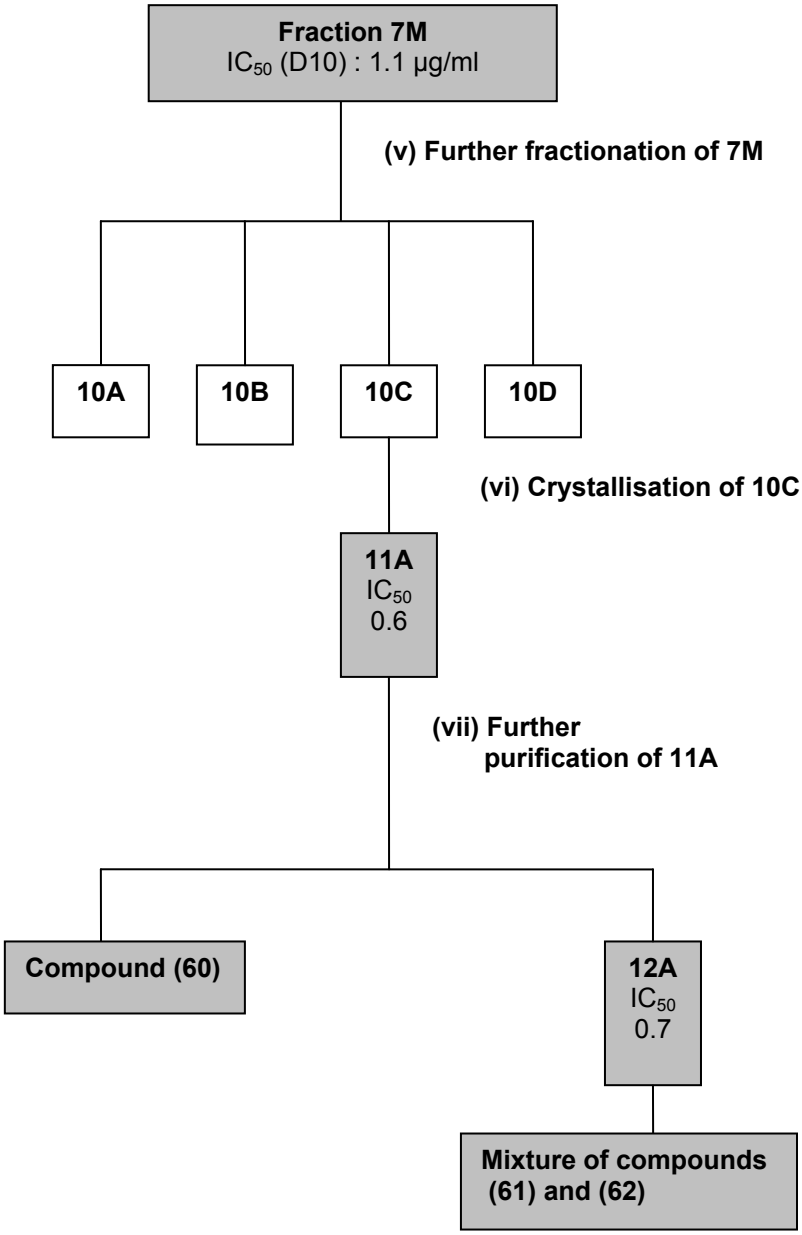

Figure 4.4 Further purification of fraction 7M. IC_{50} values are in µg/ml

4.3.4 Further Purification of Fraction 7O

Fraction 7O was found to contain one major compound, easily discernible by its dark pink colour on TLC with vanillin spray reagent. Further purification of 7O led to the isolation of the crystalline compound **(63)** (Figure 4.5). Although the yield of **(63)** was sufficient for structural elucidation and bioassaying, it was anticipated that more would be required for further characterization and thus a targeted purification of this compound from a larger quantity of crude extract was also deemed necessary.

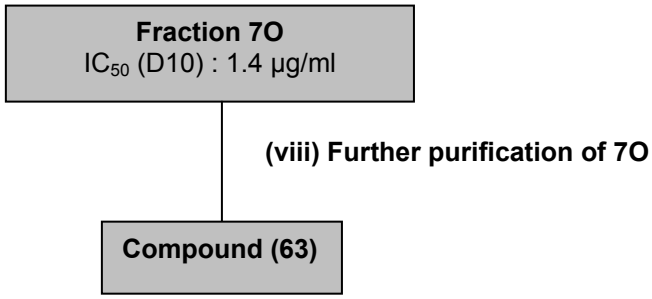

Figure 4.5 Further purification of fraction 7O. IC_{50} values are in µg/ml

4.4 Targeted Purification of Compounds (59)-(63) from P01609A

Bioassay guided fractionation of the dichloromethane extract P01609A, led to the identification of at least 5 structurally related compounds responsible for the observed activity of this extract. It was evident, however, that less active analogues of these compounds were present in the crude extract and that the overall antiplasmodial activity of the extract and several of the fractions generated were due to the synergistic effect of a number of compounds. Purification was, however, focused on those fractions showing significant enrichment of antiplasmodial activity upon fractionation so as to isolate the compounds primarily responsible for the observed biological activity. Also, low yields and marked instability rendered isolation of additional compounds from active fractions impractical.

To isolate sufficient quantities of compounds **(59)**–**(63)** for structural elucidation, characterization and bioassaying the dichloromethane extract was subjected to targeted purification techniques. Liquid-liquid partitioning of the crude dichloromethane extract once again served to concentrate the active components in a simpler matrix and proved to be an efficient method for targeting the isolation of these compounds.

TLC analysis of the three fractions generated from liquid/liquid partitioning of the crude extract revealed that the target compounds were concentrated in the dichloromethane-soluble fraction, 13B, which was then fractionated. The target compounds, identified by their characteristic R_f values and colours on TLC, were found to be present in three of the fractions generated (14B, 14E and 14F). Figure

4.6 summarises the steps employed to isolate additional quantities of compounds **(59)**, **(60)**, **(61)**, **(62)** and **(63)** for structure elucidation, derivatisation and bio-assaying. Details of the purification techniques are given in Chapter 5 (Experimental).

Compound **(59)** was isolated from fraction 14B by successive flash silica gel purifications. Once isolated, **(59)** was again observed to be unstable during NMR analysis. The acetate of **(59)**, compound **(64)**, was subsequently prepared and proved to be more stable and structure elucidation was conducted on this derivative. More material was subsequently isolated from a sub-fraction of 14B to prepare the crystalline *p*-nitrobenzoate ester of compound **(59)**, compound **(65),** for its characterization by X-ray crystallography.

Compounds **(60)**, **(61)** and **(62)** were isolated from fraction 14E by a series of crystallisations and flash silica gel purifications. The acetate of **(62)**, compound **(66),** was prepared in order to compare its X-ray structure with that of the original compound.

Compound **(63)** was isolated from fraction 14F by flash silica gel chromatography. The (*R*)- and (*S*)-Mosher ester [α-methoxy-α-trifluoromethylphenylacetate or MTPA] derivatives of **(63),** compounds **(67)**-**(72),** were prepared to determine the absolute configuration of the stereogenic centers bearing hydroxyl groups. The sodium borohydride ($NaBH_4$) reduction of **(63)** produced compound **(73)**, which was prepared to investigate a structure-activity relationship.

In contrast to a yield of almost 3% by weight of the dichloromethane extract for compound **(63),** the yields of compounds **(59)**, **(60)**, **(61)** and **(62)** were relatively low. This indicated that the antiplasmodial component was a minor constituent of the aerial parts of the plant. The low yield of compound **(59)** could be attributed to the fact that it was relatively unstable and showed evidence of decomposition during silica gel purification and on standing. The yields of all the compounds identified could possibly be improved to some extent by optimising the extraction and separation procedures. Despite the low yields the quantities of compounds

(59)–**(63)** isolated were sufficient for structure elucidation, selected derivatisations and *in vitro* assaying.

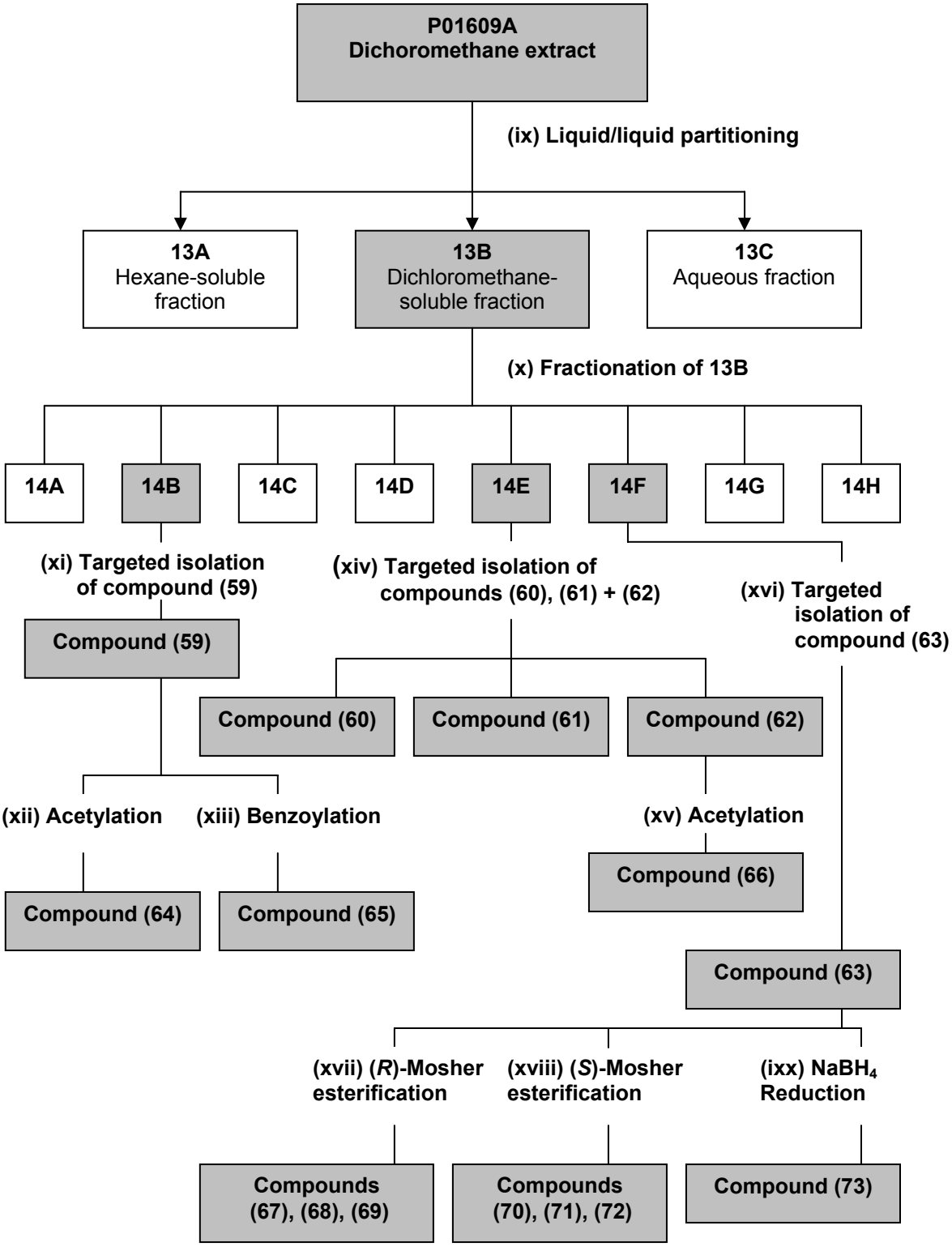

Figure 4.6 Summary of targeted purification and selected derivatisation of compounds **(59)**–**(63).**

4.5 Identification and Characterization of Compounds (59)–(63) from *O. piluliferum*

Compounds **(59)**–**(63)** were identified and characterized by mass spectrometry, specific rotation, melting points, X-ray crystallography, selected derivatisations, and ^{1}H, ^{13}C, DEPT, HSQC, HMBC, COSY and NOESY NMR experiments (as discussed in section 3.5).

4.5.1 Structure Elucidation of 4,5*α*-epoxy-6*α*-hydroxy-1(10)*E*,11(13)-germacradien-12,8*α*-olide (59).

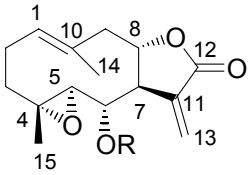

(59) R = H

(64) R = Ac

(65) R = 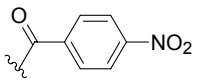

Compound **(59)** was isolated as a transparent gum. The compound showed a tendency to deteriorate on standing and this was most evident by the decomposition observed during NMR analysis. For this reason a complete set of NMR data for structure elucidation of **(59)** was not obtained. The ^{1}H NMR data of **(59)** are summarised in Table 4.4. The acetate of **(59)** was prepared and proved to be more stable, thus structural elucidation was completed on this derivative.

Compound **(64)** was obtained as a yellow gum, $[\alpha]_D$ +41.2 (*c* 0.34, $CHCl_3$). Attempts at crystallisation were unsuccessful. The ^{1}H spectrum of **(64)** revealed that a single hydroxyl group had been acetylated. The high resolution EI-MS showed an ion at *m/z* 264.1313, corresponding to the $[M - (CH_2{=}C{=}O)]^+$ fragment, which is typical of an acetate functionality. The fragment ion at *m/z* 246.1224 $[M - (CH_2{=}C{=}O) - H_2O]^+$ was also indicative of the initial loss of the ketene group. On the basis of this the molecular formula of **(64)** was deduced to be $C_{17}H_{22}O_5$.

The ^{1}H, ^{13}C, HSQC, HMBC, COSY and NOESY data of **(64)** are summarized in Table 4.5. Many of the NMR resonances were broad and unresolved and several obvious HSQC and HMBC contours were weak or undetected. Comparison with published data[3,4,5] and a few significant correlations, however, identified **(64)** as a germacranolide and facilitated its complete structural elucidation.

The C(13) (δ_C 127.27T) protons of **(64)** appeared as a pair of double doublets at δ_H 5.78 and 6.34 typical of the signals of an α-methylene-γ-lactone functionality. This was substantiated by HMBC correlations linking H(13) to C(11) (δ_C 134.33S), C(7) (δ_C 43.96D) and the lactone carbonyl carbon atom, C(12) (δ_C 168.85S). The H(13) protons showed both geminal ($J_{13,13}$ 0.7 Hz) and allylic coupling ($J_{7,13}$ ~2 Hz).

The H(7) signal (δ_H 3.00) was broadened but its multiplicity was supported by cross peaks in the COSY spectrum with H(6), H(8), H(13a) and H(13b). The one-bond correlations for H(6) (δ_H 5.23, dd, $J_{5,6}$ 3.7 Hz, $J_{6,7}$ 11.5 Hz) and H(8)(δ_H 4.48) and the signals in the HSQC spectrum at δ_C 69.25D and 77.53D, respectively, identified C(6) and C(8). The chemical shift values pointed to the presence of an oxygen atom at each of these carbon atoms. In the ^{1}H spectrum of the parent compound **(59)** (Table 4.4) the H(6) signal appeared more downfield at δ_H 4.08. This downfield shift observed for the C(6) proton on acetylation located the *O*-acetate group at C(6) (δ_C 69.25D). This was confirmed by the HMBC correlation between H(6) and the acetate carbonyl carbon atom at δ_C 168.89S. It therefore follows that the C(8) (δ_C 77.53D) oxygen atom is involved in lactone formation as shown in **(64 i)**.

Analysis of the ^{1}H NMR spectrum revealed that the H(6) signal at δ_H 5.23 (dd, $J_{5,6}$ 3.7 Hz, $J_{6,7}$ 11.5 Hz) was coupled to both H(7) and H(5). The latter signal

[3] F. Bohlmann, J. Jakupovic, M. Ahmed and A. Schuster, *Phytochemistry*, 1983, **22**, 1623.
[4] F. Bohlmann, A. Alder, J. Jakupovic, R.M. King and H. Robinson, *Phytochemistry*, 1982, **21**, 1349.
[5] F. Shafizadeh and N.R. Bhadane, *Phytochemistry*, 1973, **12**, 857.

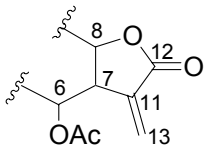

(64 i)

appeared as a doublet at δ_H 2.64 ($J_{5,6}$ 3.7 Hz). In addition HMBC correlations linked H-6 to the signals at δ_C 59.58S [C(4)] and δ_C 62.28D [C(5)]. The chemical shift values for C(4) and C(5) pointed to the presence of an oxygen atom at both these carbon atoms. The magnitude of the one-bond (^{1}H,^{13}C) coupling constant, $^1J(^1H,^{13}C)$ of 164 Hz in the coupled ^{13}C spectrum of **(64)** is typical of an epoxide methine carbon atom and established the presence of a 4,5-epoxide moiety.

Two additional HMBC correlations for the C(4) signal were observed: the one with a singlet resonating at δ_H 1.23, H(15), indicated that there was a methyl group at C(4) and the second with the protons at δ_H 1.17 and δ_H 2.03, assigned as H(3a) and H(3b), respectively. C(3) (δ_C 37.39) in turn, showed an HMBC correlation with H(2), which appeared as a broad multiplet at δ_H 2.28 and integrated for two protons. Although C(2) (δ_C 23.49T) showed no HMBC correlations, a cross peak in the COSY spectrum linked H(2) to another broad multiplet at δ_H 5.31 assigned to H(1). These results identify the fragment **(64 ii).**

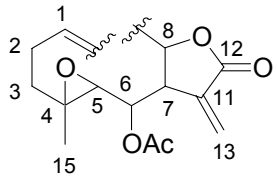

(64 ii)

The chemical shift of H(1) and the corresponding carbon atom C(1) (δ_C 127.84D) suggested that these atoms formed part of a double bond and more specifically a trisubstituted double bond. This was confirmed by the HMBC correlations between C(1) and the broad singlet at δ_H 1.72 [H(14)], which in turn was correlated to the olefinic tertiary carbon, C(10) (δ_C 129.99S). The C(14) (δ_C 19.65Q) resonance was weak and appeared as a broad hump in the ^{13}C spectrum. The absence of an

NOE between H(1) and H(14) pointed to the *E* configuration for the 1(10) double bond.

The remaining ^{1}H resonances, two broad double doublets at δ_H 1.92 and 2.82 were assigned to the C(9) protons. The corresponding carbon atom, C(9), appeared as a weak broad signal at δ_C 43.04T although no HSQC correlations were detected linking these resonances. No HMBC correlations were detected for C(9) either. The COSY spectrum did, however, indicate that the C(9) protons were coupled to each other as well as to a broad signal at δ_H 4.48, identified as H-8. This assignment completed the elucidation of the 10-membered ring of **(64)**, identifying it as a 12,8-germacranolide with an acetate at C(6), a 4,5-epoxide and a 1,10-double bond.

The relative stereochemistry of **(64)** is based on the observed coupling constants and NOE correlations and by comparison with published data.[6] Based on the Karplus equation,[7] the magnitude of the coupling constant between H(6) and H(5) (J 3.7 Hz) suggests a dihedral angle of approximately 40°. This was supported by the observed NOE correlation between H(5) and H(6). Similarly, the coupling constant between H(6) and H(7) (J 11.5 Hz) and the absence of an NOE correlation between these two protons suggests that H(6) and H(7) are antiperiplanar. Furthermore, the lactone ring fusion was shown to be trans by the absence of an NOE between H(7) and H(8) whereas the NOE observed between H(6) and H(8) indicated that both these hydrogen atoms are on the same side of the 10-membered ring. Since the configuration of H(7) is generally α in sesquiterpene lactones from higher plants;[8] H(5), H(6) and H(8) must be β-orientated. Further NOE correlations indicated that H(3a) and H(9b) were β-orientated, while H(3b) and H(9a) were α-orientated. The stereochemistry of **(64)** was thus assigned as 4,5*α*-epoxy-6*α*-hydroxygermacra-1(10)E, 11(13)-dien-12,8*α*-olide.

---

[6] F. Bohlmann and C. Zdero, *Phytochemistry*, 1977, **16**, 776.
[7] R.J. Abraham, " Introduction to NMR spectroscopy.", John Wiley & Sons, Essex, 1988.
[8] E.J. Park and J. Kim, *Planta Med.*, 1998, **64**, 752.

The *p*-nitrobenzoyl ester of **(59)** was prepared in order to obtain crystals suitable for characterisation by X-ray crystallography. The derivative **(65)** proved to be highly unstable and this not only resulted in a poor yield but also foiled attempts to recrystallize the recovered product in order to obtain crystals suitable for X-ray analysis. The ^{1}H NMR data of **(65)** are summarised in Table 4.4.

Compound **(59)** was ultimately identified as 4,5*α*-epoxy-6*α*-hydroxy-1(10)*E*, 11(13)-germacradien-12,8*α*-olide, a compound previously isolated from *Artemisia arbuscula* and *A. tridentata* as well as *Mikania pohli.* The authors of these reports depicted the epoxide moiety as 4*α*,5*β*-orientated which is impossible. The reports did, however, substantiate the observed instability of **(59)**.

Table 4.4 ^{1}H data (in $CDCl_3$) for 4,5*α*-epoxy-6*α*-hydroxy-1(10)E,11(13)-germacradien-12,8*α*-olide **(59)** and the 6-*O*-*p*-nitrobenzoyl derivative **(65)**

	(59)	**(65)**
Proton	**δ_H (J in Hz)**	**δ_H (J in Hz)**
H-1	5.33 (br m*)	5.39 (br m*)
H-2	2.30 (br m*)	2.36 (br m*)
H-3a	1.23 (dm*) (J 12.2)	1.26 (br m*)
H-3b	2.07 (ddd) (J 12.8, 3.5, 4.1)	2.10 (ddd) (J 13.0, 3.8, 4.0)
H-5	2.32 (br d*)	2.85 (br d*)
H-6	4.08 (dd) (J 3.6, 10.8)	5.59 (dd) (J 3.8, 11.5)
H-7	2.85 (br m*)	3.25 (dm*) (J 12.3)
H-8	4.42 (br m*)	4.63 (br dm*) (J 10.3)
H-9a	1.98 (br dd*)	2.02 (br dd*)
H-9b	2.85 (br dd*)	2.94 (br dd*) (J 12.0)
H-13a	6.13 (br m*)	5.77 (dd*) (J 1.6)
H-13b	6.41 (dd) (J 1.1, 2.5)	6.35 (dd*) (J 2.4)
H-14	1.74 (s)	1.83 (s)
H-15	1.40 (s)	1.48 (s)
p-nitro-Bz	-	8.16 – 8.33

* broadened signals: multiplicities and J's could not be determined

Table 4.5 ^{1}H and ^{13}C NMR data (in $CDCl_3$) for 6*α*-acetoxy-4,5*α*-epoxy-1(10)E, 11(13)-germacradien-12,8*α*-olide **(64)**

Atom	^{1}H δ_H (J in Hz)	^{13}C δ_C	HMBC $^{13}C \leftrightarrow {}^{1}H$	COSY $^{1}H \leftrightarrow {}^{1}H$	NOESY $^{1}H \leftrightarrow {}^{1}H$
1	5.31 (br m*)	127.84 D	H(14)	H(2)	H(3a); H(9a); H(2);H(7), H(8)
2	2.28 (br m*)	23.49 T		H(3a); H(1)	H-3(a); H(1)
3	H(3a) 1.17 (ddd) (J 9.5, 12.8, 10.5) H(3b) 2.03 (m#)	37.39 T	H(15), H(2), H(1)	H(3b), H(2) H(3a)	H(3b), H(2), H(5) H(3a)
4		59.58 S	H(6), H(3), H(15)		
5	2.64 (d) (J 3.7)	62.28 D	H(6), H(3b), H(15)	H(6)	H(3a), H(8), H(6), H(1)
6	5.23 (dd) (J 3.7, 11.5)	69.25 D	H(5), H(13)	H(5), H(7)	H(5), H(8)
7	3.00 (br dddd*) (J 11.5, 2.1, 2.3)	43.96 D	H(13), H(6)	H(6), H(8), H(13)	H(3b), H(1)
8	4.48 (br ddd*) (J 11.3)	77.53 D	H(6)	H(9), H(7)	H(14), H(5), H(9b), H(6), H(1)
9	H(9a) 1.92 (br dd*) (J 12.6) H(9b) 2.82 (dd) (J 12.6, 11.3)	43.04 T		H(9b), H(8) H(9a), H(8)	H(9b), H(7), H(1) H(9a), H(8)
10		129.99 S	H(14)		
11		134.33 S	H(13), H(6)		
12		168.85 S	H(13)		
13	H(13a) 5.78 (dd) (J 0.7, 2.1) H(13b) 6.34 (dd) (0.7, 2.4)	127.27 T		H(13b), H(7) H(13a), H(7)	H(13b) H(13a)
14	1.72 (br s)	19.65 Q			
15	1.23 (s)	15.81 Q	H(3a)		
6-O-CO**CH**$_3$	2.02 (s)	20.55 Q			
6-O **C**OCH$_3$		168.89 S	H(6), 6-OCOC**H**$_3$		

* broadened signals: all J's could not be determined

\# overlap with acetate peak

4.5.2 Structure Elucidation of 1*β*,6*α*-dihydroxy-4(15),11(13)-eudesmadien-12,8*α*-olide (60)

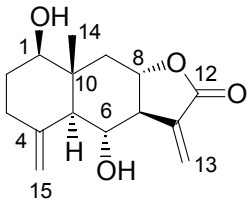

(60)

Compound **(60)** was obtained as colourless crystals, mp 278 - 280 ºC, $[\alpha]_D$ +2.0 (*c* 0.49, MeOH). The high resolution EI-MS of **(60)** showed the molecular ion peak at *m/z* 264.1347 which corresponds to a molecular formula $C_{15}H_{20}O_4$. The ^1H, ^{13}C, HSQC, HMBC, COSY and NOESY data of **(60)** are summarized in Table 4.6. The resonances of **(60)** were sharper and better resolved then was the case for (**59**), and suggested that **(60)** was structurally related to compound **(59)**. The ^{13}C spectrum of (**60**) confirmed that it had a C_{15}-skeleton, typical of germacranolide type sesquiterpene lactones.

The ^1H NMR of **(60)** exhibited four olefinic proton signals. The downfield pair of double doublets (J ~3 Hz, J 1.4 Hz) at δ_H 5.93 and δ_H 5.98 were identified as the C(13) protons, characteristic of the α-methylene-γ-lactone functionality. The upfield pair of signals at δ_H 4.83 and 4.98 were assigned to the exocyclic methylene protons H(15a) and H(15b), respectively, and both signals correlated with the δ_C 145.32S signal which is thus assigned to C(4) of the exocyclic methylene group. The H(15) signals were broadened due to both geminal coupling (J ~1 Hz) and allylic coupling (J ~1 Hz) with H(3) and H(5).

The multitude of HMBC correlations for C(5) (δ_C 57.90D) and C(10) (δ_C 43.70S), particularly those linking both these carbons to H(1), H(14), H(9) and H(6) indicated that a carbon-carbon bond existed between C(5) and C(10). Compound **(60)** was subsequently identified as an eudesmanolide with a 12,8-lactone ring.

The fragments at *m/z* 246 $[M - H_2O]^+$ and 228 $[M - H_2O - H_2O]^+$ suggested the presence of two hydroxyl functions. The two hydroxyl protons, represented by the doublets at δ_H 3.83 (J 5.3 Hz) and δ_H 3.70 (J 5.8 Hz) showed cross peaks in the

COSY spectrum with H(1) (δ_H 3.56) and H(6) (δ_H 4.13) and were consequently assigned as 1-OH and 6-OH, respectively. H(1), H(6) and H(8) were all identified and interpreted as ABX systems although some overlap of signals occurred. For instance, H(1) appeared as a dt due to coupling with H(2a) (J 11.3 Hz) and two similar couplings with H(2b) (J 5.1 Hz) and 1-OH (J 5.3 Hz). Likewise, in theory H(7) (δ_H 2.60) should be a dddd signal but appeared as a ddt due to vicinal coupling with H(8) (J 11.2 Hz) and H(6) (J 9.8 Hz) and almost equivalent allylic coupling with both H(13a) (J 3.1 Hz) and H(13b) (J 3.2 Hz).

The relative stereochemistry of **(60)** followed from comparison with compound **(64)** and published data.[9,10] The magnitude of the coupling constant of H(6) with H(5) ($J_{5,6}$ 9.9 Hz) and H(7) ($J_{6,7}$ 9.8 Hz) suggests a antiperiplanar relationship between them. The *trans* relationship between H(7) and H(8) followed from the magnitude of the coupling constant ($J_{7,8}$ 11.2 Hz). These relative configurations were confirmed by the observed NOE correlation between H(5) and H(7) and that between H(6) and H(8). As established for **(64)**, H(7) and H(5) are most likely α-orientated,[8] therefore H(6) and H(8) must be β-orientated.

The configurations at C(1) and C(10) followed from the NOEs observed between H(5) and H(1) and those between H(14), H(6) and H(8). Further NOESY correlations defined H(9b) (δ_H 2.46) and H(2a) (δ_H 1.60) as β-orientated and H(9a) (δ_H 1.53) and H(2b) (δ_H 1.82) as α-orienated. The stereochemistry of **(60)** was assigned as 1*β*,6*α*-dihydroxy-4(15),11(13)-germacradien-12,8*α*-olide.

The X-ray structural investigation of **(60)** confirmed its structure and relative stereochemistry. The conformation shown in Figure 4.7 is for the enantiomer with the lower Flack parameter. The crystals were orthorhombic and the structure was found to have the P $2_12_12_1$ space group. The cyclohexane system adopts a full chair conformation despite the sp^2 hybridization at C(4). The 4,15-*exo*-methylene group and the methyl group at C(10) are both located on the β-face and adopt an axial orientation, while both the hydroxyl groups lie in a *pseudo*-equatorial position

[9] M.L Cardona, I. Fernández, B. Garcia and J. R. Pedro, *J. Nat. Prod.*, 1990, **53**, 1042.
[10] J. Triana, M. López, M. Rico, J. González-Platas, J. Quintana, F. Estévez, F. Léon and J. Bermejo, *J. Nat. Prod.*, 2003, **66**, 943.

to minimise transannular interactions. Crystallographic data for **(60)** are tabulated in *Appendix (A)*.

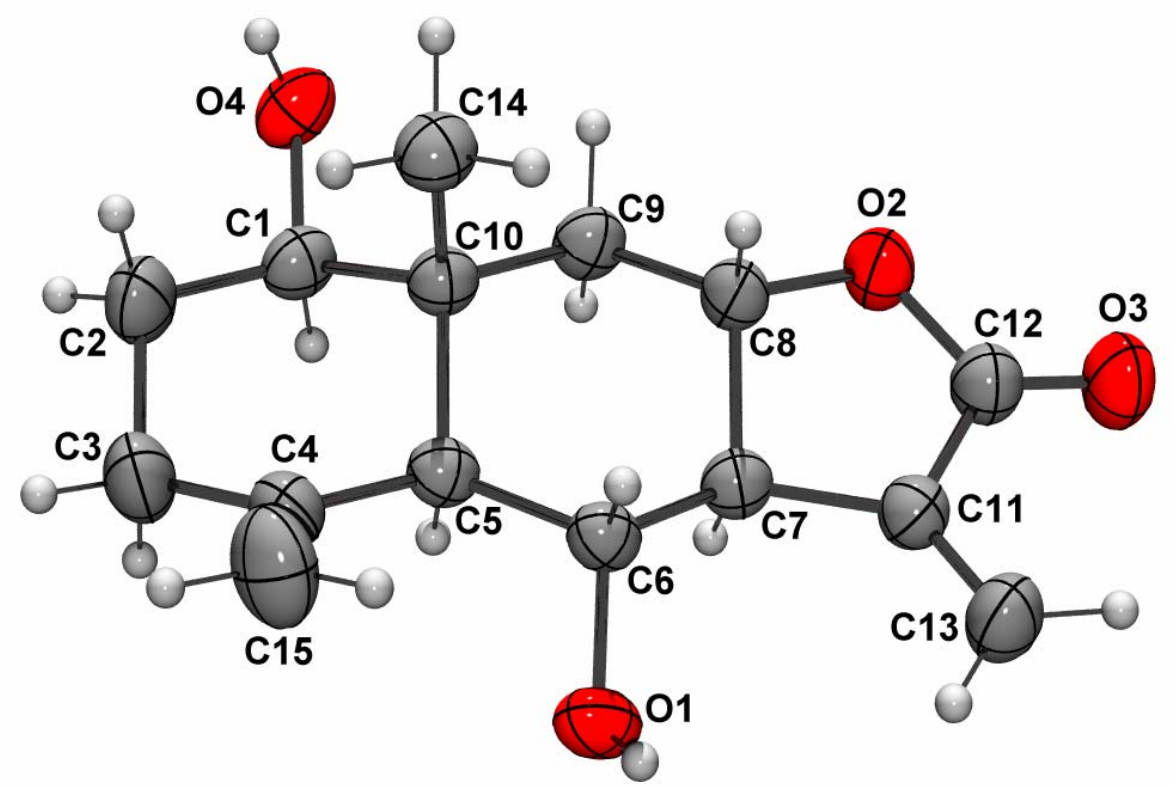

Figure 4.7 X-ray crystal structure of **(60)**

Compound **(60)** was identified as desacetyl-*β*-cyclopyrethrosin previously isolated from several other plant species such as *Mikania pohlii* and *Brocchia cinerea*.[11] The ^{1}H NMR data reported in this dissertation compared well with those reported for this compound.[9]

[11]J. Jakupovic, M.A. Aad, F. Eid, F. Bohlmann, S. El-Dahmy and T. Sarg., *Phytochemistry*, 1988, **27**, 2219.

Table 4.6 ^{1}H and ^{13}C NMR data (in acetone-d_6) for 1*β*,6*α*-dihydroxy-4(15),11(13)-eudesmadien-12,8*α*-olide **(60)**

Atom	^{1}H δ_H (J in Hz)	^{13}C δ_C	HMBC $^{13}C \leftrightarrow {}^{1}H$	COSY $^{1}H \leftrightarrow {}^{1}H$	NOESY $^{1}H \leftrightarrow {}^{1}H$
1	3.56 (ddd) (J 11.3, 5.1, 5.3)	78.51 D	H(14), H(2), H(3), 1-O**H**	H(2a), H(2b), 1-O**H**	H(9a), H(2b), H(5)
2	H(2a) 1.60 (dddd) (J 11.3, 12.9, 13.4, 5.3) H(2b) 1.82 (dddd) (J 2.0, 5.1, 12.0, 12.9)	32.54 T	H(3), H(1), 1-O**H**	H(1), H(2b), H(3b), H(3a) H(3b), H(1), H(2a)	H(14), H(2b) H(1), H(2a)
3	H(3a) 2.09 # H(3b) 2.30 (ddd) (J 2.0; 5.3; 13.4)	35.63 T	H(2), H(5), H(15)	H(2a),H(2b), H(3b),H(15b) H(2b), H(3a), H(2a)	H(3b) H(3a), H(15b)
4		145.32 S	H(2b), H(3), H(5), H(6), H(15)		
5	2.01 (br d) (J 9.9)	57.90 D	H(14), H(3), H(15), H(9b), H(1); 6-O**H**; H(6)	H(6), H(15a)	H(7), H(1)
6	4.13 (ddd) (J 5.8, 9.9; 9.8)	68.00 D	6-O**H**;H(5), H(7), H(8)	6-O**H**, H(5), H(7)	H(14), H(15a)
7	2.60 (dddd) (J 3.1, 3.2, 9.8, 11.2)	55.66 D	H(9),H(6),H(5), 6-O**H**, H(13)	H(13a), H(13b), H(6), H(8)	H(9a), H(5)
8	4.03 (ddd) (J 3.7, 11.2, 12.2)	77.65 D	H(9), H(7), H(6)	H(9b), H(7), H(9a)	H(14); H(9b)
9	H(9a) 1.53 (dd) (J 11.7, 12.2) H(9b) 2.46 (dd) (J 11.7; 3.7)	41.41 T	H(14), H(7), H(1)	H(9b), H(8) H(9a), H(8)	H(9b), H(7), H(1) H(14), H(9a), H(8)
10		43.70 S	H(15), H(9), H(2), H(6), H(1), 1-O**H**		
11		140.26 S	H(7), H(6), H(8), H(13)		
12		170.74 S	H(13)		
13	H(13a) 5.93(dd) (J 3.1; 1.4) H(13b)	118.75 T	H(7)	H(13b), H(7) H(13a), H(7)	

	5.98 (dd) (J 3.2; 1.4)				
14	0.84 (s)	14.20 Q	H(9), H(5), H(1)		H(9b), H(6), H(8), H(2a)
15	H(15a) 4.83 (br m*) H(15b) 4.98 (br m*)	109.36 T	H(3), H(6)	H(5), H(15b) H(3a), H(15a)	H(15b), H(6) H(15a)
1-O**H**	3.83 (d) (J 5.3)			H(1)	
6-O**H**	3.70 (d) (J 5.8)			H(6)	

obscured by solvent signal

* allylic coupling of ~1 Hz

4.5.3 Structure Elucidation of 1*β*,6*α*-dihydroxy-3,11(13)-eudesmadien-12,8*α*-olide (61)

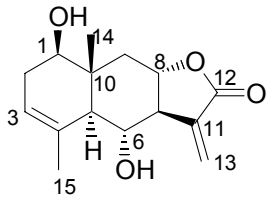

(61)

Compound **(61)** was isolated as white crystals, mp 234 - 236 ºC, $[\alpha]_D$ –38.5 (*c* 0.39, MeOH). A molecular ion peak at *m/z* 264.1261 was observed in the high resolution EI-MS of **(61)**, analyzing for $C_{15}H_{20}O_4$. Initial inspection of the ^1H and ^{13}C spectra of **(61)**, indicated that it was a close analogue of **(60)**. Thorough analysis of the ^1H, ^{13}C, HSQC, HMBC, COSY and NOESY data of **(61)**, summarized in Table 4.7, confirmed that it was also a 12,8*α*-eudesmanolide with an exocyclic double bond conjugated with the lactone carbonyl group.

The appearance of the C(3) (δ_C 122.34D) proton as a broad multiplet at δ_H 5.28 and its HMBC and COSY correlations with a broad methyl signal at δ_H 1.90, led to the deduction that there was a 3,4-double bond and a methyl group at C(4) (δ_C 134.83S). The signals were broadened due to allylic coupling of ~1Hz.

The fragments at *m/z* 246 $[M - H_2O]^+$ and 228 $[M - H_2O - H_2O]^+$ pointed to the presence of two hydroxyl groups in **(61)**. Although both C(1) (δ_C 75.14D) and C(6)

(δ_C 69.10D) are oxygen-bearing carbon atoms only the 1-OH proton resonance, represented by the doublet (J 5.4 Hz) at δ_H 3.79, could be observed. Closer inspection of the complex multiplet between δ_H 3.98 and 4.10 indicated that the H(8), H(6) and 6-OH signals overlapped. Addition of D_2O to the sample simplified its ^{1}H NMR and not only resolved the H(8) and H(6) signals but also simplified the H(6) and H(1) signals and enabled their analysis.

The observed NOESY correlations and proton-proton couplings similar to those described for **(60)**, led to the stereochemical assignments of compound **(61)**. The H(7), H(5), H(1), H(2b) and H(9a) protons were all defined as *α*-orientated, and as a consequence the H(6), H(3), H(15), H(2a), H(15), H(9b) and H(8) protons must be β-orientated. Thus **(61)** was identified as 1*β*,6*α*-dihydroxy-3,11(13)-eudesma-dien-12,8*α*-olide.

The low yield and poor crystals of **(61)** meant that no X-ray crystallography was conducted on this compound. A literature search revealed that **(61)** is a known compound commonly called sivasinolide and first isolated from *Tanacetum densum* subsp. *sivasicum.*[12] The ^{1}H NMR data of **(61)** are in agreement with published data for sivasinolide.[12]

Table 4.7 ^{1}H and ^{13}C NMR data (in acetone-d_6) for 1*β*,6*α*-dihydroxy-3, 11(13)-eudesmadien-12,8*α*-olide **(61)**

Atom	**^{1}H δ_H (J in Hz)**	**^{13}C δ_C**	**HMBC ^{13}C↔^{1}H**	**COSY ^{1}H↔^{1}H**	**NOESY ^{1}H↔^{1}H**
1	3.64 (ddd) (J 5.4, 7.0, 9.5)	75.14 D	H(14), H(2), H(3),1-O**H** H(9)	H(2a), 1-O**H**	H(2b), H(5)
2	H(2a) 1.95 (m) H(2b) 2.33 (m)	33.31 T	 H(3), 1-O**H**	H(1), H(2b) H(1), H(2a)	H(14), H(2b) H(1), H(2a), H(3)
3	5.28 (br m*)	122.34 D	H(2), H(5), H(15)	H(2b), H(15)	H(2b), H(15)
4		134.83 S	H(2b), H(5), H(6), H(15)		
5	2.13 (br dm*)	54.10 D	H(14), H(15),	H(6)	H(7), H(1),

[12] N. Gören, C. Bozak-Johansson, J. Jakupovic, L. Lin, H. Shieh, G. A. Cordell and N. Celik, *Phyto-chemistry*, 1992, **31**, 101.

	(J 10.0)		H(9b), H(1), 6-O**H**, H(6)		6-O**H**
6	4.02 (ddd) (J 8.7, 10.0, 9.8)	69.10 D	6-OH, H(5), H(7), H(8)	H(5)	H(14), H(15)
7	2.51 (dddd) (J 3.1, 3.2, 9.8, 11.5)	56.42 D	H(9), H(6), 6-O**H**, H(8), H(13)	H(13a), H(13b), H-6, H(8)	H(9a), H(5)
8	4.07 (ddd) (J 3.7, 11.5, 12.1)	77.0 D	H(9), H(7)	H(9b), H(7), H(9a)	H(14), H(9b), H(15)
9	H(9a) 1.40 (dd) (J 11.8, 12.1) H(9b) 2.41 (dd) (J 11.8, 3.7)	39.59 T	H(14), H(5)	H(9b), H(8) H(9a), H(8)	H(9b), H(7) H(14), H(9a) H(8)
10		40.91 S	H(14), H(9), H(2b), H(1), 1-O**H**		
11		139.54 S	H(7), H(6), H(8)		
12		170.02 S	H(13)		
13	H(13a) 5.91(dd) (J 3.1; 1.2) H(13b) 5.94 (dd) (J 3.2; 1.2)	117.63 T	H(7)	H(13b), H(7) H(13a), H(7)	
14	0.87 (s)	12.40 Q	H-9a,b; H-5		H-9b; H-6;H-8; H-2a; 1-OH
15	1.90 (br m*)	23.28	H(10)	H(3)	H(3)
1-O**H**	3.79 (d) (J 5.4)			H(1)	H(14)
6-O**H**	4.07 (d) (J 8.7)			H(6)	H(5)

* allylic coupling of ~1 Hz

4.5.4 Structure Elucidation of 1*α*,6*α*-dihydroxy-4*E*,9*Z*,11(13)-germacratrien-12,8*α*-olide (62)

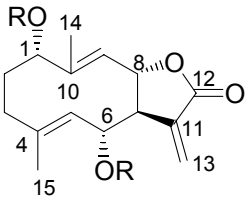

(62) R = H
(66) R = Ac

Compound **(62)** was obtained as white needles, mp 158 - 160 ºC, $[\alpha]_D$ –54.0 (*c* 0.50, MeOH). The high resolution EI-MS of **(62)** showed the molecular ion peak at *m/z* 264.1293 which established the molecular formula as $C_{15}H_{20}O_4$. Analysis of the ^1H, ^{13}C, HSQC, HMBC, COSY and NOESY data of **(62)** (see Table 4.8) revealed that it was a germacranolide with a 12,8-lactone ring, an exocyclic double bond conjugated with the lactone carbonyl group, two hydroxyl groups at C(1) and C(6), and two endocyclic double bonds at C(4) and C(9).

The presence of two hydroxyl groups was confirmed by the fragments at *m/z* 246 $[M - H_2O]^+$ and 228 $[M - H_2O - H_2O]^+$. The two one-proton doublet signals at δ_H 3.83 (J 4.1 Hz) and δ_H 4.14 (J 4.7 Hz) showed cross peaks in the COSY spectrum with H(1) (δ_H 4.39) and H(6) (δ_H 4.48), respectively, and were thus assigned as the 1-OH and 6-OH groups. These doublets were absent from the ^1H NMR spectrum (Table 4.9) of the diacetate derivative **(66)**.

The position of the 4,5-endocyclic double bond followed from the observed HMBC correlations between the methyl resonance, H(15) (δ_H 1.74) and the two signals at δ_C 133.15S and 131.31D assigned to C(4) and C(5), respectively, as well as the cross peaks in the COSY spectrum between H(15) and the methine proton H(5) (δ_H 4.93). Likewise, the position of the 9,10-endocyclic double bond followed from the correlations of H(14) (δ_H 1.76) and H(9) (δ_H 5.24) with C(9) (δ_C 126.46D) and C(10) (δ_C 142.87S). The observed multiplicities and broadening of the respective proton resonances is due to allylic coupling and further supported the assign-ments. The stereochemistry of the endocyclic double bonds was deduced from the observed NOESY correlations between the signals of H(9) and H(14) and by the

absence of an NOE between H(5) and H(15). The double bonds were therefore assigned as 4,5-(*E*) and 9,10-(*Z*).

The C(6) configuration and the trans fusion of the lactone ring was deduced from the observed proton-proton coupling constants and NOE correlations in the same way as for compounds **(59)**, **(60)** and **(61).** The assignment of the C(1) configuration was more difficult. The coupling constants of H(1) with the vicinal C(2) protons (J 10.5 and 4.8) indicate an antiperiplanar relationship between H(1) and one of the protons H(2a) or H(2b), *i.e.* an axial orientation of H(1). The conformation of germacrene derivatives, however, is often very difficult to determine due to the flexibility of medium sized rings.[13] An axial orientation of H(1) can be reached with either of the two possible configurations at C(1).

The NOESY spectrum of the acetylated derivative **(66)** in C_6D_6, however, showed a definite correlation between the H(1) and H(8) signals. Inspection of a molecular model revealed that this NOE could only be observed if the acetate group at C(1) was *α*-orientated *i.e.* C(1) has the *S* configuration . The alternative 1*R* configuration demands considerable transannular tension in order to bring H(1) and H(8) into close proximity.

Compound **(62)** was recrystallised to give trigonal crystals (detailed crystallographic data are tabulated in *Appendix (B)*). The X-ray crystal structure of **(62),** space group P 3_2, confirmed the *α*-orientation of both hydroxyl groups as well as the stereochemistry of the double bonds. The structure is illustrated in Figure 4.8 and shows that the molecule adopts a boat-chair conformation, with C(14) below and C(15) above the plane of the ring. This geometry is supported by the distinct NOE observed between H(6) and H(15).

The crystal structure revealed that there are four equivalent molecules in the asymmetric unit as well as one molecule of water. The water molecule and both the hydroxyl groups are each involved in two hydrogen bonds. The packing is such that there are empty channels running through the structure parallel to the *c* axis

[13] J.F. Sanz and J.A. Marco, *J. Nat. Prod.*, 1991, **54**, 591.

(Figure 4.9). The water molecule of each asymmetric unit lies on the edge of the channel.

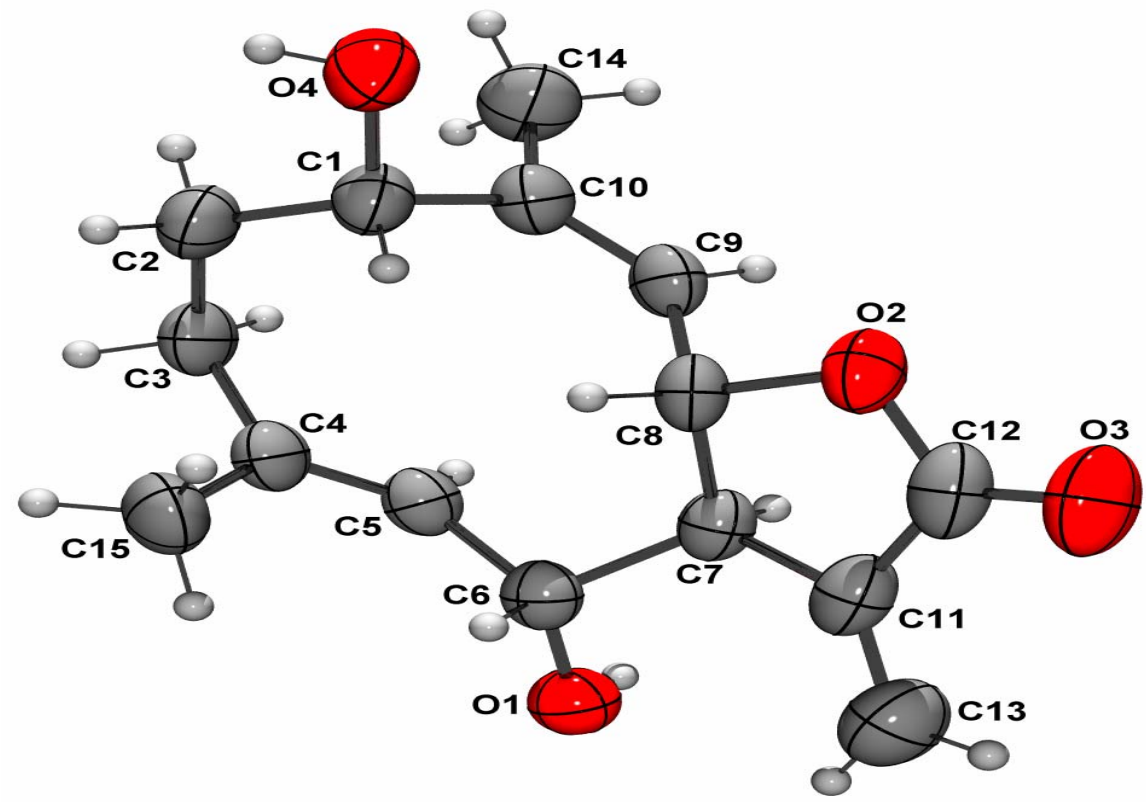

Figure 4.8 X-ray structure of **(62)**

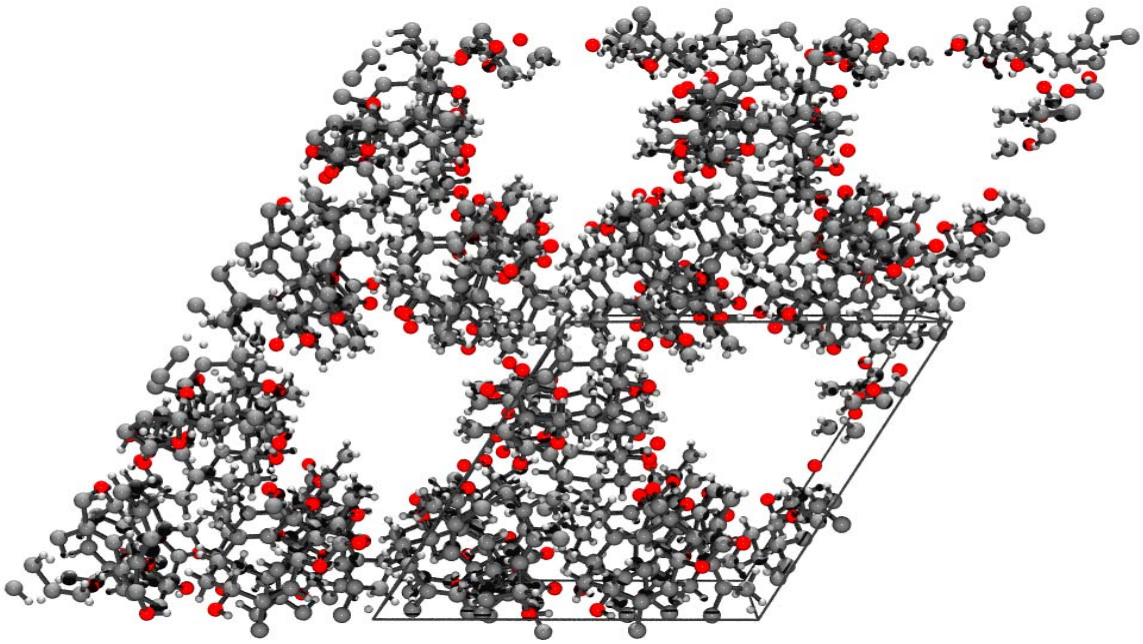

Figure 4.9 Packing of the molecules of **(62)**

To confirm that the channels are due to optimization of the H-bonds, an X-ray analysis was carried out on the diacetate derivative **(66)** which, as expected, did not show any channels. The crystals of **(66)**, space group P 2_1, were found to be monoclinic (Figure 4.10) (*Appendix (C)*).

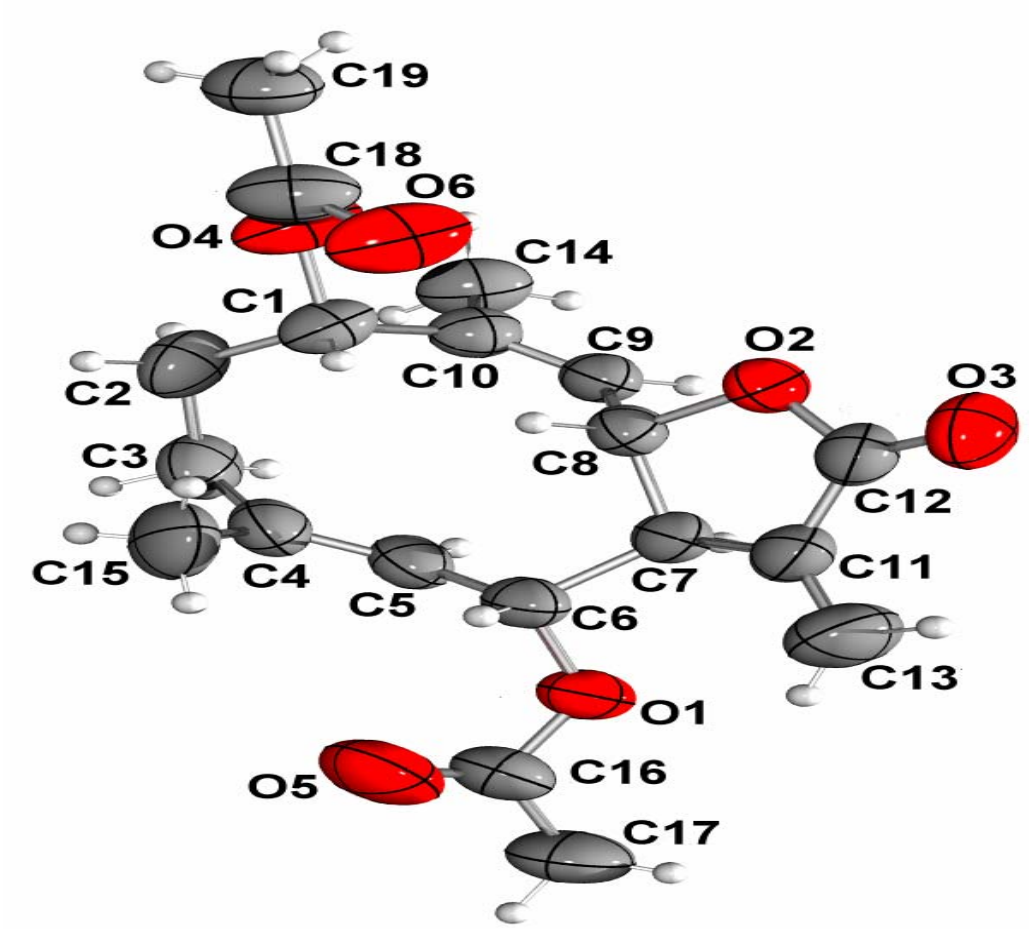

Figure 4.10 X-ray structure of **(66)**

The structure of **(62)** corresponds to tatridin A (also known as tavulin) which has been isolated from a number of plant species including *Artemisia tridentata* and *A. arbuscula* as well as *Tanacetum vulgare*.[14] The structure of **(62)** as 1*α*,6*α*-dihydroxy-4*E*,9*Z*,11(13)-germacratrien-12,8*α*-olide was confirmed by comparison of its ^{1}H, ^{13}C NMR and physical constants with published data for tatridin A.[13]

[14] A.I. Yunusov, G.P. Sidyakin and A.M. Nigmatullaev, *Khim. Prir. Soedin.*, 1979, **1**, 101.

Table 4.8 ^{1}H and ^{13}C NMR data (in acetone-d_6) for 1*α*,6*α*-dihydroxy-4*E*,9*Z*,11(13)-germacratrien-12,8*α*-olide **(62)**

Atom	^{1}H δ_H (J in Hz)	^{13}C δ_C	HMBC $^{13}C \leftrightarrow ^{1}H$	COSY $^{1}H \leftrightarrow ^{1}H$	NOESY $^{1}H \leftrightarrow ^{1}H$
1	4.39 (ddd) (J 4.1, 4.8, 10.5)	65.99 D	H(3), H(9),1-O**H**, H(2)	1-O**H**, H(2a), H(2b)	H(15), H(2)
2	H(2a) 1.67 (m) H(2b) 1.93 (m)	27.89 T	H(3), 1-O**H**, H(1)	H(1), H(2b), H(3a) H(1), H(2a), H(3)	H(2b) H(2a)
3	H(3a) 1.89 (ddd) (J 12.3; 12.4; 5.9) H(3b) 2.20 (m)	35.40 T	H(2), H(5), H(15)	H(3b), H(2a), H(2b) H(3a), H(2)	H(3b) H(3a), H(5)
4		133.15 S	H(3), H(6), H(15)		
5	4.93 (br d) (J 10.5)	131.31 D	H(15), H(3), H(7)	H(6), H(15)	H(7), H(3a)
6	4.48 (ddd) (J 4.7, 10.5, 8.8)	70.55 D	6-O**H**, H(7), H(8)	6-O**H**, H(5), H(7)	H(15)
7	2.75 (dddd) (J 3.5, 3.2, 8.8, 9.0)	52.60 D	H(9), H(6), 6-OH, H(8), H(13), H(5)	H(13b), H(13a), H(6), H(8)	H(9), H(5)
8	4.60 (dd) (J 9.0, 10.0)	74.4 D	H(7)	H(7), H(9)	H(15)
9	5.24 (br dq) (J 10.0, 1.4)	126.46 D	H(14), H(7), H(1), H(8)	H(8), H(14)	H(14), H(7)
10		142.87 S	H(14), H(8), H(2b), 1-O**H**		
11		139.76 S	H(7), H(6), H(13)		
12		170.02 S	H(13)		
13	H(13a) 5.94 (dd) (J 3.2; 1.7) H(13b) 6.03 (dd) (J 3.5, 1.7)	120.91 T	H(7)	H(7), H(13b) H(7), H(13a)	
14	1.76 (d) (J 1.4)	16.36 Q	H(9), H(1)	H(9)	H(9)
15	1.74 (br s)	14.84 Q	H(5), H(3)	H(5)	H(1), H(6), H(8)
1-O**H**	3.83 (d) (J 4.1)			H(1)	
6-O**H**	4.14 (d) (J 4.7)			H(6)	

Table 4.9 ^{1}H data (in $CDCl_3$) 1*α*,6*α*-diacetoxy-4*E*,9*Z*,11(13)-germacratrien-12,8*α*-olide **(66)**

Proton	δ_H (J in Hz)
H-1	5.44#
H-2a	1.67
H-2b/3a	1.8-2.0#
H-3b	2.29 (br m*)
H-5	4.87 (br d) (10.5)
H-6	5.41#
H-7	3.01 (br m*)
H-8	4.75 (dd) (J 9.8, 9.8)
H-9	5.36#
H-13a	5.71 (br dd*)
H-13b	6.25 (br dd*)
H-14	1.80 (br m*)
H-15	1.93 (s)
-O-COC**H**$_3$	2.00 (br s)
	2.06 (br s)

* broadened signals, all J's could not be determined
\# peaks obscured due to overlap

4.5.5 Structure Elucidation of 1*α*,6*α*-dihydroxy-4*E*,10(14),11(13)-germacratrien-12,8*α*-olide (63)

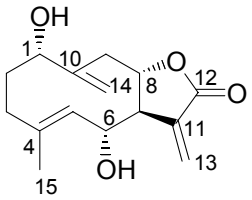

(63)

Compound **(63)** was isolated as colourless crystals, mp. 159 - 161 ºC, $[\alpha]_D$ +24.0 (*c* 0.50, MeOH). The high resolution EI-MS did not show a molecular ion peak for **(63)**, but a $[M - H_2O]^+$ fragment at *m/z* 246.1219 and a second fragment at *m/z* 228.1169 $[M - H_2O - H_2O]^+$ confirmed the presence of two hydroxyl groups and pointed to a $C_{15}H_{20}O_4$ molecular formula. The ^{1}H, ^{13}C, HSQC, HMBC, COSY and NOESY data of **(63)**, summarized in Table 4.10, suggested that it was a close analogue of compound **(62)**.

Subsequent analysis of the NMR data led to the deduction that **(63)** was also a germacranolide with a 12,8-lactone ring, an exocyclic double bond conjugated with

the lactone carbonyl, two hydroxyl groups at C(1) and C(6), and a 4,5-(*E*) endocyclic double bond. The C(4) (δ_C 134.80S) resonance was weak and broadened and was only detected when the ^{13}C spectrum was run with a delay of 3 seconds between pulses.

The only major difference between the structure of compound **(62)** and compound **(63)** was that the latter lacked a 9,10-endocyclic double bond but had a second exocyclic methylene group at C(10). The C(9) (δ_C 42.25T) protons resonating at δ_H 2.45 and δ_H 2.79, arbitrarily assigned as H(9a) and H(9b), respectively, were linked by HMBC correlations to the lactone carbon atom, C(8) (δ_C 79.66D) and the allylic carbons, C(10) (δ_C 148.62S) and C(14) (δ_C 113.77T). Cross peaks in the COSY spectrum indicated the geminal relationship between the C(9) protons (J = 14.2 Hz) as well as vicinal coupling between H(9) and H(8) (δ_H 4.60), with J = 9.6 and 2.3 Hz.

In addition, H(9b) shows allylic coupling (J~2 Hz) with the pair of broadened signals resonating at δ_H 5.06 and δ_H 5.10, corresponding to the exocyclic methylene protons, H(14a) and H(14b). This was supported by the observed multiplicities of the H(9a) (dd) and H(9b) (dddd) proton signals, which were analysed using the ^1H NMR spectrum of **(63)** in $CDCl_3$ (Table 4.11), where these signals appeared more defined and better resolved than in acetone-d_6. The coupling of only H(9b), and not H(9a), with the C(14) protons suggests that it is in the same plane as the π-system. Observed coupling constants and NOESY correlations with H(8) indicate that H(9b) is *β*-orientated, while H(9a) is *α*-orientated. NOE correlations between H(9b), H(14) and the methyl resonance at δ_H 1.70, H(15), indicate that in solution they are all on the same side of the cyclodecane ring *i.e*. they are *β*-orientated.

Contrary to this, the X-ray structure analysis of **(63)** showed that the methyl and methylene groups at C(4) and C(10) are *anti* (Figure 4.11). Apart from this, it was confirmed that the lactone ring was linked with the germacrane ring in a trans manner and that the 2 hydroxyl groups were *α*-orientated. The crystals were orthorhombic and the structure was found to have the P $2_12_12_1$ space group. The

10-membered ring adopts a boat-boat conformation. The hydroxyl groups are maintained in a pseudo-equatorial position, away from the inner part of the ring to minimize transannular interactions. Detailed crystallographic data for **(63)** are tabulated in *Appendix (D)*.

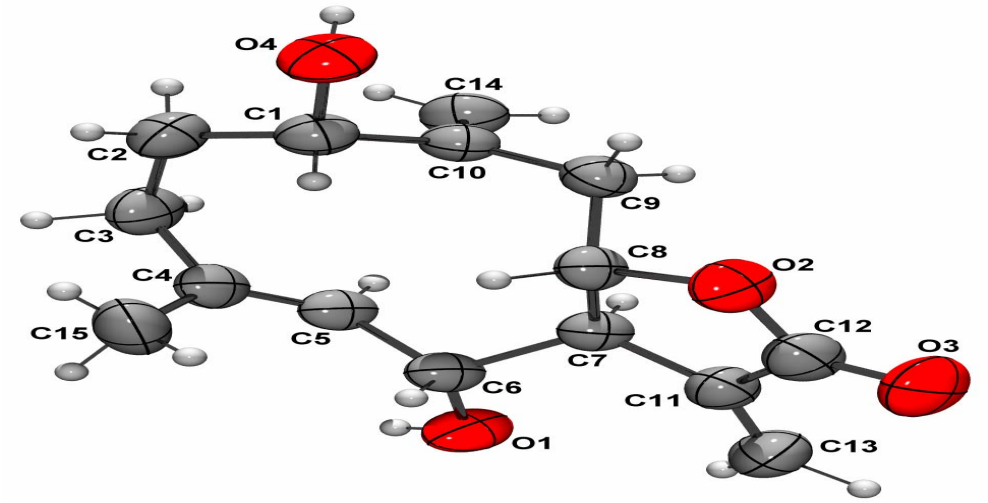

Figure 4.11 X-ray structure of **(63)**

Compound **(63)** was identified as tanachin, first isolated from *Tanacetum pseudoachillea*[15]. This compound has subsequently been isolated from a variety of plants in the *Asteraceae* family in Middle Asia.[12,13,16] The identification of **(63)** as 1*α*,6*α*-dihydroxy-4E,10(14),11(13)-germacratrien-12,8*α*-olide was confirmed by comparison of its ^{1}H, ^{13}C NMR and physical constants with published data for tanachin.[17]

Table 4.10 ^{1}H and ^{13}C NMR data (in acetone-d_6) for 1*α*,6*α*-dihydroxy-4*E*, 10(14),11(13)-germacratrien-12,8*α*-olide **(63)**

Atom	^{1}H δ_H (J in Hz)	^{13}C δ_C	HMBC $^{13}C\leftrightarrow{}^{1}H$	COSY $^{1}H\leftrightarrow{}^{1}H$	NOESY $^{1}H\leftrightarrow{}^{1}H$
1	3.90 (ddd) (J 6.2, 10.3, 4.4)	70.35 D	H(3), H(9), 1-O**H**, H(2), H(14)	1-O**H**, H(2a), H(2b)	H(15), H(9b), H(8), H(14)
2	2.03 (m)	31.89 T	H(3), 1-O**H**, H(1)	H(1), H(3)	
3	H(3a) 2.01 (m)	35.06 T	H(2), H(5), H(15)	H(3b), H(2)	

[15] A.I Yunusov, N.D. Abdullaev, S.Z. Kasymov and G.P. Sidyakin., *Khim. Prir. Soedin.*, 1976, **2**, 263.
[16] M.B. Izbosarov, Kh. T. Zairova, B. Kh. Abduazimov, V.M. Malikov, *Khim. Prir. Soedin*, 2000, **36**, 288.
[17] A.I.Yunusov, N.D. Adbullaev, Sh. Z. Kasymov, G.P. Sidyakin and M.R. Yagudaev, ., *Khim. Prir. Soedin.*, 1976, **4**, 462.

	H(3b) 2.24 (m)			H(3a), H(2)	H(5), H(14)
4		134.80 S	H(3), H(6), H(15), H(2)		
5	5.07 (br dd) (J 9.9, 1.4)	132.91 D	H(15), H(3), H(6), 6-O**H**	H(15), H(6)	H(9a), H(7)
6	4.31 (ddd) (J 4.4, 9.9, 9.5)	70.99 D	6-O**H**, H(7), H(5)	6-O**H**, H(5), H(7)	H(15), H(8)
7	2.82 (dddd) (J 2.8, 3.2, 6.6, 9.5)	52.82 D	H(9), H(6), 6-O**H**, H(8), H(13)	H(13a), H(13b), H(8), H(6)	H(13a), H(5), H(9a)
8	4.60 (br ddd) (J 6.6, 9.6, 2.3)	79.66 D	H(7), H(9), H(6)	H(7), H(9a), H(9b)	H(15), H(1), H(6), H(9b), H(14)
9	H(9a) 2.45 (dd) (J 9.6, 14.2) H(9b) 2.79 (dddd) (J 2.3, 14.2, 2.0; 2.0)	42.25 T	H(14), H(7), H(1)	H(8), H(9b) H(8), H(9a), H(14a), H(14b)	H(5), H(7) H(1), H(14), H(8), H(15)
10		148.62 S	H(14), 1-OH, H(1), H(9), H(2)		
11		139.27 S	H(7), H(6), H(13)		
12		170.11 S	H(7), H(13)		
13	H(13a) 6.12 (dd) (J 2.8, 1.4) H(13b) 6.16 (dd) (J 3.2; 1.4)	132.77 T	H(7)	H(7), H(13b) H(7), H(13a)	H(7)
14	H(14a) 5.06 (br d) (J 2.0) H(14b) 5.10 (br s)	113.77 T	H(9), H(1)	H(9b)	H(1), H(8), H(9b), H(15)
15	1.70 (d) (J 1.4)	14.84 Q	H(5), H(3)		H(1), H(6), H(8), H(14), H(9b)
1-O**H**	3.68 (d, 6.2)			H(1)	
6-O**H**	4.14 (d, 4.4)			H(6)	

Table 4.11 ^{1}H data (in $CDCl_3$) for 1*α*,6*α*-dihydroxy-4*E*,10(14),11(13)-germacratrien-12,8*α*-olide **(63)**

Proton	δ_H (J in Hz)
H-1	3.81 (ddd) (J 4.6, 10.3, 6.3)
H-2a/b	2.00 (m*)
H-3a	1.95 (m*)
H-3b	2.17 (m*)
H-5	5.00 (br dd) (J 9.8, 1.4)
H-6	4.19 (ddd) (4.3, 9.8, 9.6)
H-7	2.74 (dddd) (J 9.6, 6.6, 2.8, 3.2)
H-8	3.90 (br m*)
H-9a	2.31 (dd) (J 9.6, 14.2)
H-9b	2.82 (dddd) (14.2, 2.0, 1.9, 2.3)
H-13a	6.13 (dd) (1.4, 2.8)
H-13b	6.17 (dd) (1.4, 3.2)
H-14a	4.99 (br d) (J 1.8)
H-14b	5.04 (br s)
H-15	1.61 (d) (J 1.4)
1-OH	3.10 (d) (J 6.3)
6-OH	3.58 (d) (J 4.3)

* broadened signals, all J's could not be determined

4.5.6 Characterization of Compounds (59) – (63)

Compounds **(59)**, **(62)** and **(63)** were identified as germacranolides by their lactone and cyclodecane rings, as well as the exocyclic double bond conjugated with the lactone carbonyl. They were characterised as germacrane lactones with a linear structure due to the α,β-unsaturated lactone being fused to the C(8)-C(7) positions of the carbocyclic skeleton. Similarly, compounds **(60)** and **(61)** were identified as the linear germacranolide derivatives, known as eudesmanolides, distinguished by the cyclodecane ring being split into two six membered rings by a C(5)-C(10) bond. All the compounds were further characterized by the position and

stereochemistry of hydroxyl groups, double bonds and, in the case of **(59)**, the epoxide moeity on the cyclodecane ring.

The presence of certain broadened, unresolved signals in the ^{1}H and ^{13}C spectra is indicative of conformational equilibria in solution. In general the 7,8-germacranolides are known to be conformationally labile. It has been shown, however, that certain conformations are hindered because of steric repulsion between the *syn*-directed C(15) methyl group and the α-OH substituent at C(6) and that transition between the more favoured conformations is determined by the conformational mobility of the C(9)-C(10)-C(1)-C(2) section.[18] The presence of a hydroxyl group at C(1) in compounds **(62)** and **(63)** therefore renders the 10-membered rings less mobile than **(59)**, for instance.

Although compounds **(59)** – **(63)** are all known compounds, having been previously isolated from a variety of plant species, this is the first report of their isolation from *Oncosiphon piluliferum* and in fact the first report on any chemical constituents of this plant. The compounds identified, however, are all sesquiterpene lactones which are common components in the *Asteraceae* family. The bitter taste of *O. piluliferum* suggests that the sesquiterpene lactone content is relatively high, and thus it is evident that several other structurally related compounds occur in the dichloromethane extract.

4.5.7 Absolute Configurations of Compounds (59)–(63)

Due to the relatively high yield of **(63)**, Mosher's method could be applied to determine the absolute stereochemistry of this compound. This technique is a empirically derived chemical method used to determine the absolute configuration of organic compounds possessing a secondary hydroxyl group.[19,20,21]

---

[18] M.K. Makhmudov, B.K. Abuazimov, B. Tashkhodzhaev and B.T. Ibragimov, *Khim. Prir. Soedin.*, 1989, **2**, 198.
[19] J.A. Dale and H.S. Mosher, *J. Am. Chem. Soc.*, 1973, **95**, 512.
[20] I. Ohtani, T. Kusumi, Y. Kashman and H. Kakisawa, *J. Am. Chem. Soc.*, 1991, **113**, 4092.
[21] M.J. Rieser, Y. Hui, K. Rupprecht, J.F. Kozlowski, K.V. Wood, J.L. McLaughlin, P.R. Hanson, Z. Zhuang and T. R. Hoye, *J. Am. Chem. Soc.*, 1992, **114**, 10203.

4.5.7.1 Mosher Esters of Compound (63)

The Mosher acid, (*R*)-*α*-methoxy-*α*-trifluoromethylphenyl acetic acid, [(*R*)-MTPA] upon treatment with thionyl chloride is converted to the *S* acid chloride [(*S*)-MTPA-Cl]. The ester formation *of* this acid chloride with a chiral alcohol then leads to the formation of the (*R*)-MTPA ester. Similarly, the *S* acid gives rise to the *S* ester via the *R* acid chloride (Figure 4.12).[21]

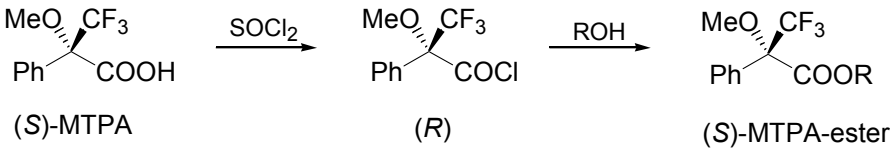

Figure 4.12 (*S*)-Mosher acid esterification of an alcohol

Since compound **(63)** has 2 secondary hydroxyl groups the (*R*)-MTPA esterification of compound **(63)** resulted in the isolation of three products, a diester and two monoesters, compounds **(67)**, **(68)** and **(69)**. Ester formation of compound **(63)** with (*S*)-MTPA produced the Mosher esters **(70)**, **(71)** and **(72)**.

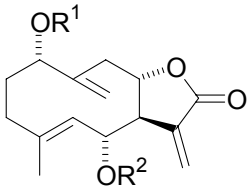

Compound	R^1	R^2
(67)	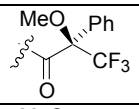	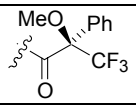
(68)	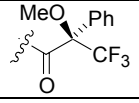	H
(69)	H	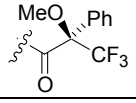
(70)	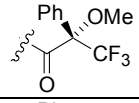	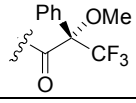
(71)	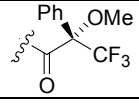	H
(72)	H	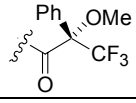

Figure 4.13 Mosher esters of compound **(63)**

4.5.7.2 Mosher's Method

Mosher's method is based on the hypothesis that MTPA ester groups exist in solution in a conformation in which the methine proton, ester carbonyl group and trifluoromethyl group lie in the same plane (Figure 4.14).

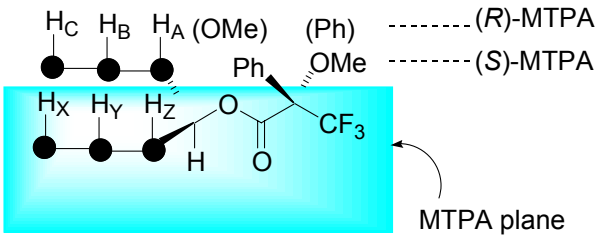

Figure 4.14 MTPA plane of an MTPA ester. $H_{A,B,C}$ and $H_{X,Y,Z}$ are on the right and left sides of the plane respectively.

Due to the diamagnetic effect of the phenyl group the $H_{A,B,C...}$ NMR signals of the (*R*)-MTPA ester should appear upfield relative to those of the (*S*)-MTPA ester. The reverse should hold true for $H_{X,Y,Z...}$. Therefore protons on the right side of the MTPA plane must have positive $\Delta\delta$ (δ_S - δ_R) values and protons on the left side of the plane must have negative values, as illustrated in Figure 4.15.[20]

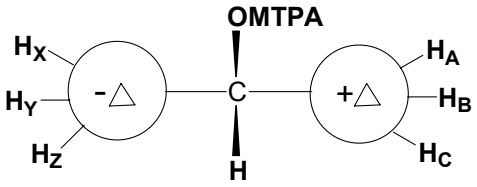

Figure 4.15 Model to determine of the absolute configuration of secondary alcohols.

4.5.7.3 Application of Mosher's Method – Absolute Stereochemistry of Compound (63)

Proton signals were assigned for each of the (R)- and (*S*)-MTPA esters of **(63)**. The COSY spectra were used to determine the approximate chemical shifts of those signals that were severely overlapped in the ^{1}H NMR spectra. $\Delta\delta$ values were obtained for the protons of the 1,6-di-*O*-MTPA derivatives, compounds **(67)** and **(70)**, the 1-*O*-MTPA derivatives, compounds **(68)** and **(71),** and the 6-*O*-MTPA derivatives, compounds **(69)** and **(72)**, of compound **(63)**. These values are summarized in Figure 4.16.

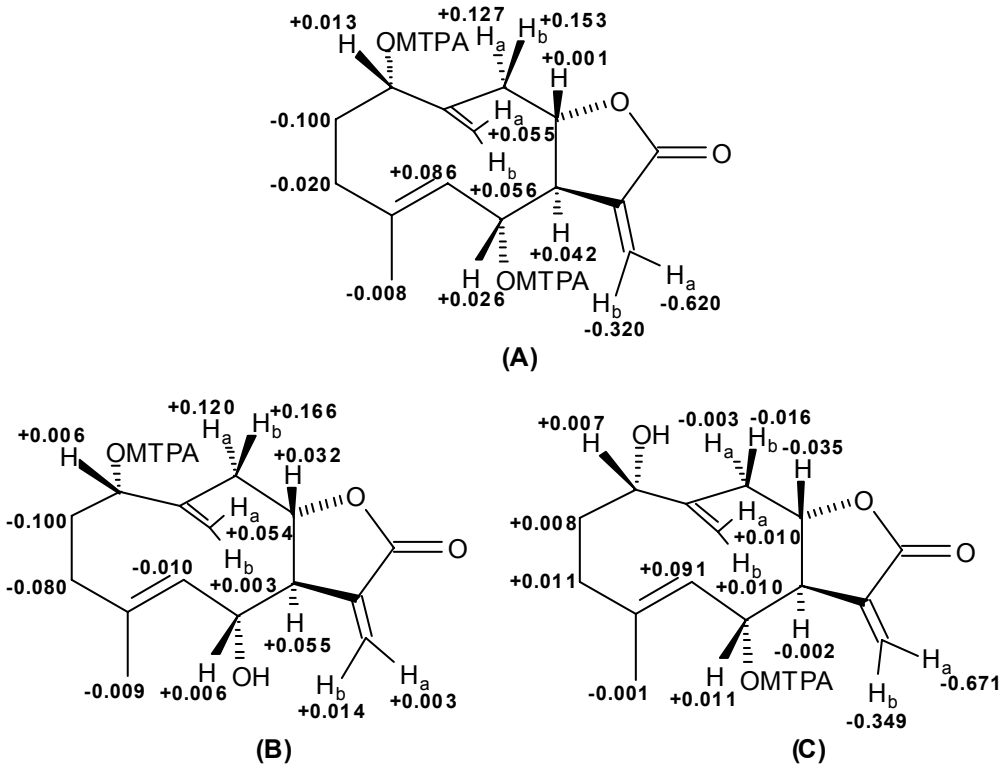

Figure 4.16 $\Delta\delta$ Values obtained for the 1,6-*O*-di-MTPA derivative **(A)**, the 1-*O*-MTPA derivative **(B)** and the 6-*O*-MTPA derivative **(C)** of compound **(63)**

Since the $\Delta\delta$ values for the H(2), H(3) and H(5) protons **(B)** are negative they are located on the left side of the MTPA plane at C(1) whereas the positive $\Delta\delta$ values for the H(14), H(9) and H(8) protons places them on the right side of the MTPA plane. Substitution of these two groups of protons into the model shown in Figures 4.14 and 4.15 and subsequent application of the Cahn-Ingold-Prelog sequence rules,[22] indicates that C(1) has the *S* configuration.

Similarly, it follows from **(C)** that the H(5), H(2) and H(3) protons are on the right side and H(7), H(8) and the H(13) protons are on the left side of the MTPA plane at C(6). The R configuration is thus assigned to C(6).

From **(A)** it can be noted that for the diesters, the $\Delta\delta$ values for the protons on either side of the MTPA plane at C(1) support the findings of **(B)**, but at C(6) the positive and negative $\Delta\delta$ values are irregularly dispersed on the left and right sides

[22] R.T. Morrison and R.N. Boyd, 'Organic Chemistry', 6th edition, Prentice Hall International, New York, 1992

of the MTPA plane. This may be due to changes in the conformation of the diester due to steric congestion around the C(6) stereogenic centre.

The absolute configuration of the other stereogenic centres, C(7) and C(8) of **(63)** followed from the established relative stereochemistry and application of the Cahn-Ingold-Prelog sequence rules, and compound **(63)** is thus (1*S*,6*R*,7*S*,8*S*)-1,6-dihydroxy-4*E*,10(14),11(13)-germacratrien-12,8-olide.

4.5.7.4 Biosynthesis of Compounds (59) – (62)

In recognizing that compounds **(59)** – **(63)** are all structurally related and have the same relative stereochemistry at C(6), C(7) and C(8) it is evident that these secondary metabolites are formed from a common biogenetic precursor. Thus the absolute stereochemistry of the other compounds can be deduced from that of **(63)**. Figure 4.17 outlines the proposed biosynthesis of **(59)** – **(63)** based on literature precedent and summarises the deduced absolute configurations.

Although the possibility cannot be ruled out, it seems unlikely that costinolide **(25)** is the biogenetic precursor of compounds **(59)** – **(63)**, as this would require not only hydroxylation of costinolide at C(8), but also the shifting of the lactone ring from C(6)-C(7) to C(7)-C(8). It appears more likely that hydroxylation occurs at C(8) of **(39),** the immediate precursor of costinolide, to give the 6,8-dihydroxy-germacratrien-12-oic acid **(74)**. The manner in which the C(6) and C(8) oxygen atoms are introduced is not known, but sufficient evidence suggests that direct oxidation of C-H to C-OH is a common biological process.[23] The less sterically hindered C(7)-C(8) lactone closure of **(74)** yields the basic sesquiterpene lactone precursor known as deacetyllaurenobiolide **(75)**. This compound is reported to have been isolated from *Tanacetum densum* concurrently with compounds **(61)** and **(63)**.[12]

[23] TA Geissman, 'The Biogenesis of Sesquiterpene Lactones of the Compositae', University of California Press, California, 1973.

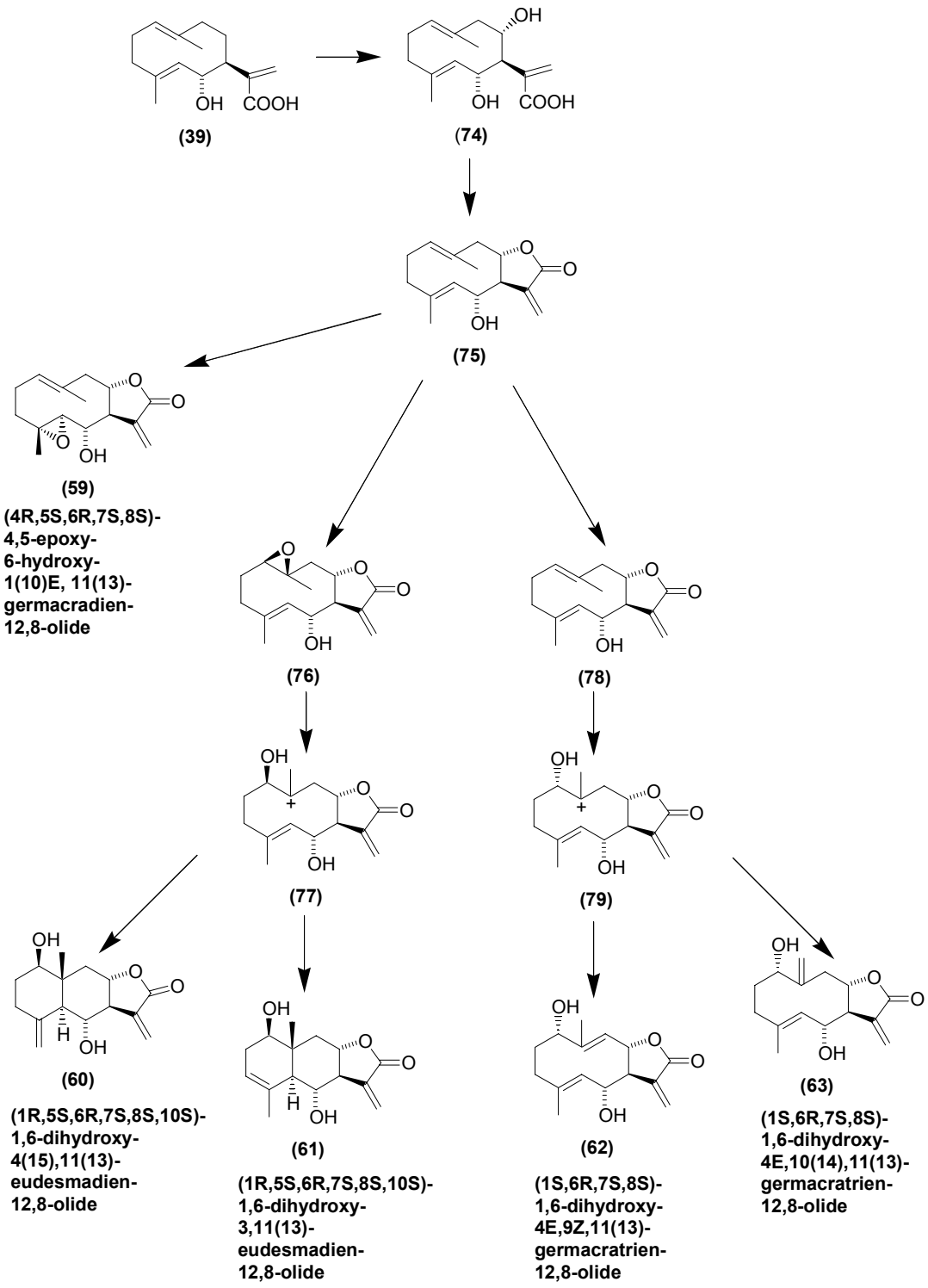

Figure 4.17 Postulated biosynthesis of compounds **(59)**, **(60)**, **(61)**, **(62)** and **(63)**

Compound **(59)** would result from the selective epoxidation of the 4,5-double bond of **(75)** from below the plane of the ring. As epoxidation is considered an important

means of introducing oxygen into natural organic compounds,[24] it is probable that the 1-OH group in compounds **(60)**, **(61)**, **(62)** and **(63)** arises from the selective epoxidation of the 1,10-double bond of **(75)**. The opposite configurations of the 1-OH groups in the eudesmanolides, **(60)** and **(61**), and the germacranolides, **(62)** and **(63)**, suggests that the epoxidation of this allylic system can occur from either face in **(75)**. Epoxidation from above the plane of the ring yields **(76)**, which upon acid-catalysed epoxide opening gives the 1β-OH intermediate cation **(77)**. Subsequent ring closure would yield the eudesmanolides **(60)** and **(61)**. Similarly epoxidation from below the plane of the ring of **(75)** yields **(78)**, which can be converted to germacranolides **(62)** or **(63)** *via* the 1*α*-OH intermediate cation **(79)**.

4.6 $NaBH_4$ Reduction of Compound (63)

Compounds **(59)**-**(63)** were all found to possess an α-methylene-γ-lactone functional group. Since it has been established that this moiety is typically responsible for the biological activity of sesquiterpene lactones,[25] an attempt was made to determine what effect the reduction of the C(11)-C(13) exocyclic double bond would have on the antiplasmodial activity and cytotoxicity of these compounds. The relatively high yield of **(63)** provided additional material to attempt the reduction of the C(11)-C(13) exocyclic double bond with $NaBH_4$ in methanol. Although the yield of the reaction was low (34%) adequate product **(73)** was recovered for characterization by NMR and bioassaying. No additional physical data could be obtained on the compound due to its instability.

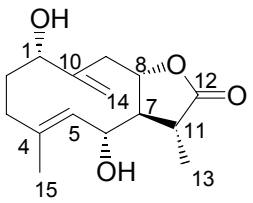

(73)

Compound **(73)** was recovered as a pale yellow gum. The ^{1}H NMR data of **(73)**, summarized in Table 4.12, clearly indicated that the *α*-methylene lactone function

[24] T.A. Geissman, *Phytochemistry*, 1970, **9**, 2377.
[25] E. Rodriguez, G.H.N. Towers and J.C. Mitchell, *Phytochemistry*, 1976, **15**, 1573.

of **(63)** had been reduced to give the 11,13-dihydro derivative and that the reaction yielded only one of the two possible stereoisomers.

The pair of doublets corresponding to those of the C(13) methylene group in **(63)** were absent from the ^{1}H NMR spectrum of **(73)** and were replaced by a methyl signal resonating at δ_H 1.39 (d, J 7.2 Hz). There was also an additional proton signal at δ_H 2.63 identified as H(11). The assignment of H(11) was supported by the observed multiplicity of this resonance which appeared as a dq due to vicinal coupling with H(7) (J 9.1 Hz) and the methyl protons, H(13) (J 7.2 Hz).

The stereochemistry at C(11) followed from the magnitude of the coupling constant between H(7) and H(11) (J 9.1Hz), which suggested an antiperiplanar relationship between them. This was confirmed by the strong NOE correlation observed between H(13) and H(7) in the NOESY spectrum of **(73)**.

The reduction of **(63)** with $NaBH_4$ in methanol therefore yielded (1*S*,6*R*,7*S*,8*S*, *11*R)-1,6-dihydroxy-11,13-dihydro-4*E*,10(14),11(13)-germacratrien-12,8-olide. The fact that the reduction resulted in only one of the possible stereoisomers was in accordance with previous reports on the reduction of related sesquiterpene lactones with $NaBH_4$.[9,26] The anion **(80)** is protonated from the less-hindered side of the enolate double bond to form the thermodynamically more stable stereo-isomer *ie*. where the new methyl group is less hindered.

[26] M.A. Irwin, K.H. Lee, R.F. Simpson and T.A. Geissman , *Phytochemistry*, 1969, **8**, 2009.

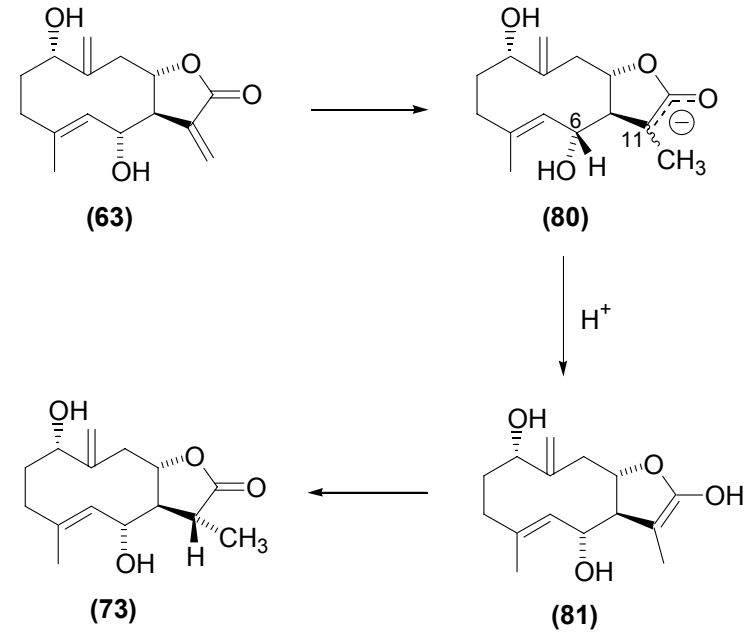

(1S,6R,7S,8S,11R)-1,6-dihydroxy-11,13-dihydro-4E,10(14)-germacradien-12,8-olide

Figure 4.19 $NaBH_4$ reduction of compound **(63).**

Table 4.12 ^1H data (in $CDCl_3$) for (1*S*,6*R*,7*S*,8*S*,*11*R)-1,6-dihydroxy-11,13-dihydro- 4*E*,10(14)-germacradien-12,8-olide **(73)**

Proton	**δ_H (J in Hz)**
H(1)	3.92 (dd) (J 4.9, 9.7)
H(2)	2.00 (m)
H(3a)	1.90 (ddd) (J 5.5, 5.7, 13.5)
H(3b)	2.06 (ddd) (J 5.5, 5.1, 8.8)
H(5)	5.10 (br d) (J 10.1)
H(6)	4.26 (dd) (J 10.1, 9.8)
H(7)	2.26 (ddd) (J 5.5, 9.1, 9.8)
H(8)	3.89 (ddd) (J 2.5, 8.3, 5.5)
H(9a)	2.41 (dd) (J 15.3, 8.3)
H(9b)	2.80 (dddd) (J 2.3, 2.2, 2.5, 15.3)
H(11)	2.63 (dq) (J 7.2, 9.1)
H(13)	1.39 (d)

	(J 7.2)
H(14a)	5.03 (br d) (J 2.2)
H(14b)	5.07 (br dd) (J 2.2, ~1)
H(15)	1.65 (d) (J 1.3)

4.7 *In vitro* Antiplasmodial Activity and Cytotoxicity of Compounds from *O.piluliferum*

Compounds **(60)**, **(61)**, **(62)**, **(63)**, **(64)** and **(73)** were tested for *in vitro* antiplasmodial against the D10 and K1 *P. falciparum* strains using the pLDH assay. The corresponding IC_{50} and RI values of chloroquine and the 6 compounds are listed in Table 4.13

Table 4.13 *In vitro* antiplasmodial activity of chloroquine, compounds **(60)** - **(64)** and compound **(73)**

Tested sample	**D10 IC_{50} (μg/ml)**	**K1 IC_{50} (μg/ml)**	**RI***
Chloroquine	11.1×10^{-3}	181.76×10^{-3}	15.36
Compound **(64)**	0.5	1.6	3.2
Compound **(60)**	4.4	4.2	1.0
Compound **(61)**	2.6	2.3	0.9
Compound **(62)**	0.4	1.0	2.5
Compound **(63)**	0.5	1.8	3.6
Compound **(73)**	70.0	ND	ND

* RI = K_1 IC_{50} / D_{10} IC_{50}

ND = Not determined

Compound **(73)** can be considered completely inactive. The germacranolides **(64)**, **(62)** and **(63)** showed equipotent antiplasmodial activity and were found to be significantly more active than the eudesmanolides **(60)** and **(61).** This is most likely due to the flexibility and conformational features of the 10-membered ring as opposed to the bi-cyclohexane ring system but the effect of other structural

features cannot be ruled out. For instance, the presence of a 4,15-exocyclic methylene group, such as that in **(60)**, has been reported to decrease antiplasmodial activity in structurally related eudesmanolides.[27] This might explain why **(60)** was the least active of the isolated compounds and why it had a higher IC_{50} than **(61)** when these two compounds differ only in the position of one double bond.

No significant conclusions could be drawn from the structure-activity relationship between the three germacranolides. In the case of compounds **(62)** and **(63)** the difference in antiplasmodial activity was minimal yet they also differ in the position of one double bond. While in compound **(62)**, C-10 has an exocyclic double bond; in compound **(63)** there is a C(9)-C(10) endocyclic double bond. Compound **(64)**, which has a 4,5-epoxide moiety, was equipotent to compounds **(62)** and **(63)** which both have a double bond in this position.

There are no previous reports of compounds **(59)** and **(60)** being investigated for any biological activity. Compounds **(61)**, **(62)** and **(63)** have been found to show antibacterial activity.[12,16] This is the first report of any of the compounds having antiplasmodial activity.

The *in vitro* cytotoxicity of the compounds against CHO cells was determined using the MTT assay. The corresponding IC_{50} and SI values of chloroquine and the 6 compounds are listed in Table 4.14

Table 4.14 *In vitro* cytotoxicity of chloroquine, compounds **(60)** - **(64)** and compound **(73)**

Tested sample	**CHO IC_{50} (μg/ml)**	**SI***
Chloroquine	18.5	1666.7
Compound **(64)**	2.2	4.4
Compound **(60)**	10.1	2.3
Compound **(61)**	4.0	1.5

[27] G. Lang, C.M. Passreiter, C.W. Wright, N.H. Filipowicz, J. Addae-Kyereme, B.E. Medinilla and J. Castillo, *Z. Naturforsch.*, 2002, **57c**, 282.

Compound **(62)**	6.0	15.0
Compound **(63)**	6.4	12.8
Compound **(73)**	>100	>1.4

* SI = cytotoxicity CHO IC_{50}/antiplasmodial D_{10} IC_{50}

All compounds, except compound **(73)**, also showed significant toxicity to CHO cells at similar concentrations and this is emphasized by their low SI values – only **(62)** and **(63)** can be considered hits based on the criteria discussed in Chapter 3.[28] The data suggests that the observed antiplasmodial activity might be due to general toxicity. The antiplasmodial and cytotoxicity assay results of compound **(73)** clearly show that the C(11)-C(13) exocyclic double bond of **(63)** is primarily responsible for both the antiplasmodial activity and toxicity to CHO cells as both are significantly decreased when this double bond is reduced. This result is in accordance with previous findings that the presence of an α-methylene-γ-lactone functional group is an active centre for cytotoxicity[29] and antiplasmodial activity.[30,31] Since compounds **(64)**, **(60)**, **(61)**, **(62)** and **(63)** all possess an α-methylene-γ-lactone moiety, one would expect that they would all show equipotent antiplasmodial activity and toxicity to CHO cells, which is clearly not the case. The fact that there are significant differences in the IC_{50} values of each compound in the two assays as well as between the various compounds suggests that there is more than just the cytotoxic effect of the α-methylene-γ-lactone group coming into play.

4.8 Conclusion and Research Prospects

Although *Oncosiphon piluliferum* is reported to have been used medicinally, it was shown here to contain structurally related sesquiterpene lactones with significant toxicity. The compounds **(59)**, **(60)**, and **(61)** did show antiplasmodial activity but their potential for development of antimalarial drugs is limited due to inherent cytotoxicity and lack of selectivity. This is often the case with antimalarial compounds identified from plants.[32] Although their activity and SI values cannot be

[28] R. Pink, A. Hudson, M. Mouriès and M. Bendig, *Nature Rev. Drug Discov.*, 2005, **4**, 727.
[29] A.K. Picman, *Biochem. Syst. Ecol.*, 1986, **14**, 255.
[30] G. Francois, C.M. Passreiter, H.J. Woerdenbag and M. Van Looveren, *Planta Med.*, 1996, 62, 126.
[31] J.D. Phillipson and C.W. Wright, *J. Ethnopharmacol.*, 1991, **32**, 155.
[32] S. Schwikkard and F.R. van Heerden, *Nat. Prod. Rep.*, 2002, **19**, 675.

compared to that of chloroquine, **(62)** and **(63)** can be considered as hits that could be subjected to more detailed analysis, involving accurate IC_{50} determinations against whole parasites, measurement of general cytotoxicity and *in vivo* assessment in animal models.

These compounds could also be used as models to generate lead compounds with enhanced antiplasmodial activity and reduced cytoxicity. One such medicinal chemistry approach would be to investigate how the addition of known biologically active moieties to the C(11)-C(13) exocyclic double bond (the cytotoxic component) would affect the antiplasmodial activity. Further structure-activity relationship studies would also help draw a conclusion as to whether the antiplasmodial activity observed for sesquiterpene lactones such as **(59)**, **(60)**, **(61)**, **(62)** and **(63)** is indeed biological activity or just the result of general cytotoxicity.